# Torsion and vibration-torsion levels of the $S_1$ and ground cation electronic states of *para*-fluorotoluene

Adrian M. Gardner, William D. Tuttle, Laura Whalley, Andrew Claydon, Joseph H. Carter and Timothy G. Wright[a]

School of Chemistry, University of Nottingham, University Park, Nottingham NG7 2RD, UK

[a] Tim.Wright@nottingham.ac.uk

## Abstract

We investigate the low-energy transitions (0–570 $cm^{-1}$) of the $S_1$ state of *para*-fluorotoluene (*p*FT) using a combination of resonance-enhanced multiphoton ionization (REMPI) and zero-kinetic-energy (ZEKE) spectroscopy and quantum chemical calculations. By using various $S_1$ states as intermediate levels, we obtain zero-kinetic-energy (ZEKE) spectra. The differing activity observed allows detailed assignments to be made of both the cation and $S_1$ low-energy levels. The assignments are in line with the recently-published work on toluene from the Lawrance group [J. Chem. Phys. **143**, 044313 (2015)], which considered vibration-torsion coupling in depth for the $S_1$ state of toluene. In addition, we investigate whether two bands that occur in the range 390–420 $cm^{-1}$ are the result of a Fermi resonance; we present evidence for weak coupling between various vibrations and torsions that contribute to this region. This work has led to the identification of a number of misassignments in the literature, and these are corrected.

## I. INTRODUCTION

Torsion, or internal rotation, occurs in many systems, but $CH_3$-containing molecules have been the focus of most attention. In particular, the role of the methyl rotor in enhancing internal energy dispersal has been of considerable interest.[1] This interest resides in the prevalence of methyl groups in biomolecules, and the possibility for the torsional motion to be coupled to particular vibrations and hence provide additional routes for energy dispersal within the molecule. In excited states, this energy dispersal is expected to lead to enhanced photostability of a molecule (see refs. 2 and 3), particularly if there is subsequent coupling to other electronic states via internal conversion (IC) or intersystem crossing (ISC). A number of key biomolecules have groups attached directly to a phenyl ring and so simple molecules which have these or similar groups are of great interest in unravelling the photophysics and photochemistry of such systems. Hence, substituted benzenes have been a particular focus of attention, with toluene being the simplest such molecule with a methyl group. In the present work, we shall provide assignments of the $S_1$ levels of *para*-fluorotoluene (*p*FT) in the region < 570 $cm^{-1}$ and discuss these in relation to those in toluene.

The $S_1 \leftarrow S_0$ transition of the toluene molecule was studied a number of times up to the year 2000, and we highlight the publications of Murakami et al.,[4] Breen et al.[5], Hickman et al.[6] and Borst and Pratt[7] (and references to additional work may be found therein). We very recently studied the toluene molecule using resonance-enhanced multiphoton ionization (REMPI) and zero-kinetic-energy (ZEKE) spectroscopy,[8,9] where we were able to assign the vibrational structure in terms of $M_i$ modes.[10] Together with contemporaneous results from two-dimensional laser-induced fluorescence (2D-LIF) experiments from Gascooke and Lawrance[11]

and earlier time-resolved photoelectron work (tr-PES) from Reid and coworkers,[12] much insight into a Fermi resonance (FR) at ~ 460 $cm^{-1}$ in the $S_1$ state was uncovered. Further work combining the results of tr-PES and ZEKE studies[9,13] also allowed insight into more complicated vibrational dynamics to higher energy.

In its simplest form, a Fermi resonance is an interaction between a single zero-order vibrational state (ZOS) that is "bright" and so carries oscillator strength, and another such state that is "dark" and carries no oscillator strength. If these are of the correct symmetry and are close in energy, then they can interact, giving rise to two eigenstates that are linear combinations of the two ZOSs; as such, both of the resulting eigenstates can be observed in a frequency-resolved spectrum, albeit at shifted energy positions. Of course, this picture can become more complicated with more than two ZOSs interacting (a "complex" Fermi resonance) and, further, it may be that more than one of the ZOSs is "bright". The interest in such interactions is that the resulting eigenstates are effectively coupling ZOS vibrational motions and, in a time-dependent picture, we can think of energy oscillating and/or flowing from one ZOS to another and so there is a redistribution of vibrational energy within the molecule – so-called intramolecular vibrational redistribution (IVR).

Recently, interacting vibration-torsion coupled states (hereafter called *vibtor* states) have been unambiguously identified in the toluene molecule by Gascooke et al.[14] In an earlier paper,[8] we reported a band in the REMPI spectra of toluene at ~ 165 $cm^{-1}$, but we had been unable to assign since it did not fit the expected position for any vibrational or torsional level. In ref. 14 it was shown by Gascooke et al., using 2D-LIF, that this band arose from a transition to an $S_1$ level that was an eigenstate arising from a pair of coupled ZOSs, one of which was a

vibtor level with the other being a pure torsional level. This coupling between states involving torsions can be viewed as a generalized form of Fermi resonance. The second component of the Fermi resonance was not conclusively observed by ourselves; however, it was noted in ref. 14 that the corresponding feature is present in the published REMPI spectrum of Doyle et al.[15] Such vibration-torsion coupling had initially been discussed for toluene in the $S_0$ state by Gascooke et al.[16] and this also allowed them to reinterpret rotationally-resolved spectra in terms of transitions involving vibtor levels.[17] There are two key conclusions from the 2D-LIF studies: first that vibration-torsion coupling leads to a direct communication between the ladders of torsional levels and the vibrational ones, thus providing a direct route for vibrational energy redistribution via vibtor states; and secondly, that the deduction of torsional parameters such as $V_6$ (see below) from spacings between observed levels needs to be treated with caution, since these can be affected by such vibration-torsional coupling. In Refs. 14 and 16 it was shown that the derived height of torsional barriers could be significantly in error if vibration-torsion interactions are not taken into account. Since knowledge of energy levels is one of the key links between the molecular level and bulk thermodynamics, and since being able to understand the energy level spacings and intensities of spectra is a key test of quantum mechanical models, it is important that these are well understood.

The work of ref. 14 updates earlier assignments of the low-energy region of the $S_1 \leftarrow S_0$ spectrum of toluene,[4,5] which had been used in other work.[8,18,19,20] In particular, we note that the torsional levels of the toluene cation have been investigated in resonant experiments, using the $S_1$ levels as intermediates. A detailed study was initially undertaken by Lu et al.[18] using ZEKE spectroscopy and although this region of the spectrum has been reported via

mass-analyzed threshold ionization (MATI) spectroscopy subsequently,[19,20] the assignments in those latter studies have merely referred back to the Lu et al. study.

The *p*FT molecule has had a very large number of studies undertaken on it. This is due to three key facts: it is one of the simplest molecules with a single torsional group; it is a substituted benzene molecule with a $S_1 \leftarrow S_0$ transition at amenable wavelengths; and finally it has a large transition dipole moment, making the spectra straightforward to observe. The available detailed analysis of the spectrum of *p*FT,[21] together with the well-understood spectrum of *para*-difluorobenzene (*p*DFB),[22] has led to a comparison between IVR rates between the two molecules having been performed in great detail over the years; in particular, we note the seminal experiments covering both chemical timing by Parmenter and coworkers[23,24,25] and picosecond tr-PES experiments by Reid and coworkers.[13,26,27,28,29] These experiments have highlighted the role played by the methyl group in accelerating IVR via vibration-torsional coupling.

Overall, we would expect the low-energy torsional region of a neutral or cationic electronic state of the *p*FT molecule to resemble closely the corresponding one of toluene; however, the low-wavenumber vibrations, which could interact with the torsional states to form vibtor levels, are likely to be at different wavenumbers in the two molecules, thus changing the couplings and so the nature of the final vibtor levels. The torsional levels of the $S_0$ and $S_1$ states of *p*FT have been investigated by LIF and dispersed fluorescence (DF) by Okuyama et al.[30] and by REMPI, LIF and DF by Zhao et al.[31,32] These levels have also been reported by Georgiev et al.[33] when examining the *p*FT-Ar complex. Of note is that Hu et al.[34] reported a very nice spectrum of the torsional region of *p*FT and used this in assigning the same region of the pFT-

Ar complex, and Zhao et al.[31] show beautiful spectra of the region < 300 $cm^{-1}$ above the origin for both *p*FT as well as the *p*FT-$d_3$ isotopologue (an earlier version of this study is also available in ref. 35). The torsional levels of the *p*FT cation have been investigated by Takazawa et al.[36] using ZEKE spectroscopy and we shall refer back to this work later.

Although we have studied the *p*FT cation previously by ZEKE spectroscopy,[37] we mostly concentrated in that work on vibrational states to higher wavenumber. However, two low-wavenumber $S_1 \leftarrow S_0$ bands were also studied and assigned to low-wavenumber vibrations by comparison with the work of Okuyama et al.[30] In the present work, we shall confirm a reassignment of these[32] as part of our present focus on the low-wavenumber region of the spectrum, for which we present newly-recorded ZEKE spectra when exciting through a significant number of intermediate $S_1$ levels < 570 $cm^{-1}$ above the origin; in addition, several levels have been incorrectly assigned to torsional levels – see below. By considering the recent results of Gascooke et al. on toluene,[14] together with the appearance of the REMPI and ZEKE spectra of *p*FT, we present assignments of the spectra. We shall briefly compare with the results from 2D-LIF studies that are described in a forthcoming paper;[38] a more detailed discussion of the torsion-vibrational couplings in the $S_0$, $S_1$ and $D_0^+$ states will form part of a further paper.[39]

In Table I we show the $D_i$ labels employed in the present study for the vibrations of *p*FT, which have been discussed in ref. 40. Also shown in Table I are Varsányi labels,[41] which confusingly do not represent the same vibrational motions as the Wilson[42] labels employed; however, unfortunately these labels have been used extensively in previous work. In contrast, the present $D_i$ labels allow the motions of the atoms to be deduced from the numbered mode

(see mode diagrams in ref. 40). Also used in a number of recent studies are Mulliken labels, but purporting to be based on the vibrations of *p*FT in the $C_{2v}$ point group; however, the numbering has included the methyl-localized vibrations, which actually cannot be classified in $C_{2v}$. We have included these labels in Table I simply to aid the reader when comparing with other studies. Also included are indications of how the $D_i$ modes can be compared to Wilson modes – the reader should refer to ref. 40 for a discussion of this (and that work will also inform the reader of how the $D_i$ labels for *para*-disubstituted benzenes relate to the $M_i$ ones for monsubstituted benzenes). Finally, in the present work we shall highlight the similarity of the spectral activity in *p*FT and *p*DFB and for this we need to use the same mode labels – made possible by the use of the $D_i$ labels[40] – and we therefore note the correspondence between these and the $D_{2h}$ Mulliken labels in Table I; again, this will prove useful to the reader when comparing different studies.

Interactions between ZOSs can be uncovered via dispersed fluorescence, as was done in ref. 14, or in principle by an ionization method, such as we shall employ in the present work for *p*FT. Indeed, the tr-PES experiments of Reid et al.[28] use such an approach and have discussed different couplings occurring for energy levels associated with different *m* levels. Unfortunately, we did not record ZEKE spectra when exciting via the 165 $cm^{-1}$ feature when we performed the toluene study,[8] but we did excite through other Fermi resonance features and their different make-up was inferred from the varying intensities in the ZEKE spectra.[8,9] In the present work, we expect many facets of the interactions in toluene to carry over into *p*FT, with the proviso that the vibrational levels are expected to shift, but that the energies of the unperturbed torsional levels should be to be very similar to those of toluene. In line with the conclusions from ref. 14, we can reasonably expect to see transitions involving vibtor

levels arising from the combination of the $m$ = 3(-) torsional level with vibrations of $b_1$ ($a_2''$) symmetry and, as will be seen, other torsional levels also may appear with vibrations of other symmetries (see Table II, and additional comments below).

## II. THEORETICAL CONSIDERATIONS

Molecules containing methyl rotors are generally considered in molecular symmetry groups[43] and for toluene and *p*FT, this is the $G_{12}$ symmetry group, which is isomorphic to the $D_{3h}$ point group.

Hindered torsional energy levels are found by solving the Schrödinger equation below, with the appropriate potential function, $V(\phi)$:

$$[-F\partial^2/\partial\phi^2 + V(\phi)]\,\psi = E\,\psi \qquad (1)$$

where $F$ is the rotational constant of the methyl rotor and $\phi$ is the torsional angle. For toluene and *p*FT, the form of the potential is:

$$V(\phi) = {}^1/_2\sum V_n(1-\cos n\phi) \qquad (2)$$

with $n$ being a multiple of 3 for methyl rotors, with the lowest term being $V_6$ for toluene and *p*FT because of their symmetry.

For a methyl group attached to an infinite mass, the energies of the internal rotor/torsional levels are given by

$$E_{tor} = \underline{m}^2 F \quad (3)$$

where $\underline{m}$ is the (integral) torsional quantum number for an unhindered rotor and each level is doubly degenerate;[16] $F$ is the rotational constant of the methyl group. In the *p*FT molecule, the torsion of the methyl group has to be counteracted by rotation of the rest of the molecule in the opposite direction, and this slightly changes the rotational constant, although this may simply be accounted for by noting that $F$ is an effective rotational constant associated with the torsional motion. Once we have hindered rotation, the $\underline{m}$ = 3 and $\underline{m}$ = 6 levels lose their degeneracy owing to the $V_6$ term and, following Gascooke et al.,[16] the internal rotor states are now represented by quantum numbers, $m$. If $m$ is not a multiple of 3, then the levels are still doubly degenerate, but could be separately referred to with a +/- sign. If $m$ is a multiple of 3, then new eigenstates are formed, which, for example, can be represented as $m$ = 3(+) and $m$ = 3(-), with the sign indicating the specific linear combination of the original $\underline{m}$ = +3 and $\underline{m}$ = -3 states. By analogy with toluene and other similar molecules,[44,45] we expect to see $\Delta m$ = 0 transitions as the most intense pure torsional transitions, followed by $\Delta m$ = 3 and then $\Delta m$ = 6 ones and so on (see below). It is also pertinent to note that the two lowest, $m$ = 0 and $m$ = 1, levels have different nuclear spin state symmetries, and hence cannot interconvert in a supersonic jet expansion, meaning that both will be populated even under the coldest conditions.[5]

At this point it is important to define the axis systems employed. For benzene, the molecule lies in the *xy* plane, with the *z* axis coincident with the $C_6$ symmetry axis. For a $D_{2h}$ molecule, the *z* axis will pass through the fluorine atoms of *p*DFB, but the protocol for selecting the *x*

and *y* axes are not so definitive. We follow the axis system employed by Knight and Kable,[46] who located the molecule in the *yz* plane. A similar issue arises with a $C_{2v}$ molecule and to be consistent with our previous work, we also locate the molecule in the *yz* plane, with the *z* axis passing through the unique (substituent) atom (or group) and the centre of the phenyl ring; this axis system is shown in Figure 1. With these axis conventions in $D_{6h}$ for benzene, the $S_1$ state is designated $\tilde{A}\,^1B_{2u}$, the $S_2$ state is $\tilde{B}\,^1B_{1u}$, and the $S_3$ state is $\tilde{C}\,^1E_{1u}$.

It is well known that owing to a Herzberg-Teller (HT) vibronic interaction, benzene and substituted benzenes display non-totally symmetric vibrations during the $S_1 \leftarrow S_0$ transition. Using point group symmetry, in the $D_{6h}$ benzene molecule, the transition to the dipole-forbidden $\tilde{A}\,^1B_{2u}$ electronic state occurs as a result of vibronic interaction with the $\tilde{C}^1E_{1u}$ excited electronic state, for which a transition is dipole-allowed. The $\tilde{A}\,^1B_{2u}$ state gains intensity via vibronic coupling via $e_{2g}$ vibrations by interacting with/stealing intensity from the $\tilde{C}^1E_{1u}$ state. Under $C_{2v}$ symmetry, the $S_1$ state is $\tilde{A}\,^1B_2$ and the next corresponding excited states are $\tilde{B}^1B_2$, $\tilde{C}^1B_2$ and $\tilde{D}^1A_1$, thus these latter three states can be vibronically coupled to the $S_1$ state via $b_2$ and $a_1$ vibrations, explaining the activity of $b_2$ vibrations in the $S_1 \leftarrow S_0$ transition of such molecules. (The correlation between the $D_{6h}$ and $C_{2v}$ point group symmetry labels is given in Figure 1.) Thus, in molecules such as toluene and *p*FT, if the methyl group is considered to be a point mass, we expect to see vibrational activity of FC-forbidden $b_2$ symmetry modes, since the electronic state which is responsible for the main HT interaction is of $A_1$ symmetry (the overall vibronic symmetry of the $S_1$ level must also be $A_1$, with the electronic symmetry being $B_2$). Note that it is also possible that $a_1$ vibrations, which are Franck-Condon (FC)-allowed, can also gain intensity via HT vibronic coupling[47,48] – this could

be evident as unexpected intensity variations within a progression,[48] or as differences in vibrational band intensities in one- and two-photon REMPI spectra.[49,50]

When we consider the torsional states, we need to note that the corresponding $C_{2v}$ point group symmetry classes correspond to the relevant $G_{12}$ molecular symmetry ones as follows: $a_1 \sim a_1'$; $b_2 \sim a_1''$; $a_2 \sim a_2'$; and $b_1 \sim a_2''$ – see Figure 1. Thus, for a torsional or vibtor level to be FC-allowed it needs to have $a_1'$ symmetry overall. Under the Born-Oppenheimer approximation, together with the assumption of complete separability of rotational, torsional and vibrational motion, we should only expect to observe $\Delta m$ = 0 or 6 torsional transitions and transitions to totally-symmetric vibrational or vibtor levels. There is also the possibility that such levels are able to interact with an $a_1'$ vibration by a generalized form of Fermi resonance as noted above. For a vibtor level to be HT active in the $S_1$ state via a generalized form of the above mechanism, it must have $a_1''$ symmetry, to give $A_1'$ overall vibration-torsion-electronic symmetry.[44] In addition, torsional, vibrational and vibtor levels that have the same symmetry may interact with each other, with the symmetry of a vibtor level being given by the direct product of the torsional and vibrational symmetries. These comments on symmetry are summarized in Table II, while in Table III we summarize the symmetries of various vibtor levels arising from the lowest wavenumber vibrations, which are pertinent to the present work.

**III. CALCULATIONAL DETAILS**

For the $S_1$ ($\tilde{A}\,^1B_2$) state TD-B3LYP/aug-cc-pVTZ calculations were undertaken, while for the $D_0^+$ ($\tilde{X}\,^2B_1$) ground state cation, UB3LYP/aug-cc-pVTZ calculations were performed, which

yielded $<S^2>$ values of ~ 0.76, indicating spin contamination was minimal. The calculated values are presented in Table I. For the $S_1$ and $D_0^+$ states of *p*FT, we find that the vibrational motions were often altered slightly from the $S_0$ motion of the $D_i$ modes, but it was always possible to identify the most appropriate $D_i$ label in each case. Such assignments will, however, not include any strong resonance effects, such as Fermi resonance; in such cases, the actual eigenfunctions will correspond to mixtures of the $D_i$ ZOS motions.

With regard to the equilibrium geometries, we optimized both eclipsed (one of the methyl CH bonds is in the plane of the phenyl ring) and staggered (one of the methyl CH bonds is perpendicular to the plane of the phenyl ring) conformation. For the $S_1$ state, the eclipsed geometry gave no imaginary frequencies, while the staggered geometry gave one imaginary frequency even though the latter was the lowest energy structure (by 20.9 $cm^{-1}$). The tabulated vibrational wavenumbers in Table I are those for the lowest energy, staggered conformer. For the $D_o^+$ state, both the eclipsed and staggered geometries gave no imaginary frequencies, but the staggered geometry was the lower in energy (by 3.3 $cm^{-1}$). The tabulated vibrational wavenumbers in Table I are thus those for the staggered conformer.

**IV. EXPERIMENTAL**

The apparatus employed has been described previously in detail elsewhere,[51] incorporating small modifications in order to perform the two-colour ZEKE experiments, which have also been described,[52] and so only a brief description is given here. For all experiments, the ionization laser was a dye laser (Sirah Cobra-Stretch) operating with Pyrromethene 597 laser dye and was pumped with the second harmonic (532 nm) of a Surelite I Nd:YAG laser. The excitation laser was a dye laser (Sirah Cobra-Stretch) operating with Coumarin 540A, and in

some cases a mixture of Coumarin 540A and Coumarin 503 was used to extend the range, and was pumped with the third harmonic (355 nm) of a Surelite III Nd:YAG laser. The fundamental frequencies produced by each dye laser were frequency doubled using BBO and KDP crystals for the pump and probe lasers, respectively.

*para*-Fluorotoluene (99% purity, Alfa Aesar) was seeded in ~1.5 bar of Ar and the gaseous mixture passed through a General Valve pulsed nozzle (750 μm, 10 Hz, opening time of 180–210 μs) to create a free jet expansion. The focused, frequency-doubled outputs of the two dye lasers were overlapped spatially and temporally and passed through a vacuum chamber coaxially and counterpropagating. Here, they intersected the free jet expansion between two biased electrical grids located in the extraction region of a time-of-flight mass spectrometer that was employed in the REMPI experiments; these grids were also used in the ZEKE experiments by application of pulsed voltages, giving fields ($F$) of ~10 V cm$^{-1}$, after a delay of up to 2 μs, where this delay was minimized while avoiding introducing excess noise from the prompt electron signal. Because of the well-known decay of the lower-lying Rydberg states accessed in the pulsed-field ionization process,[53] bands had widths of ~5-7 cm$^{-1}$, even when $\sqrt{F}$ relationships would suggest the widths should be significantly greater.

For this work, we also recorded a two-colour REMPI spectrum of *para*-difluorobenzene. For this experiment, the excitation laser was a dye laser (Sirach Cobra-Stretch) operating with Coumarin 540A and was pumped with the third harmonic (355 nm) of a Surelite III Nd:YAG laser. The ionization laser was a dye laser (Sirach Cobra-Stretch) operating with Coumarin 503, and was pumped with third harmonic (355 nm) of a Surelite I Nd:YAG laser, set at 39895.5 cm$^{-1}$ to avoid any $S_1 \leftarrow S_0$ resonances with this second colour.

## V. RESULTS AND DISCUSSION

### A. REMPI Spectrum

The REMPI spectra of *p*FT reported in the present paper and the associated 2D-LIF one[38] show very similar structure; however, simulation of the 2D-LIF band contours has allowed band origins to be determined in that work and hence more precise energy level spacings to be derived. The REMPI spectrum was calibrated to the origin transition at 36859.9 $cm^{-1}$ to be consistent with our earlier work[37] that used this value, taken from Okuyama et al.[30] The 0–570 $cm^{-1}$ region of the present $S_1 \leftarrow S_0$ REMPI spectrum is shown in Figure 2 (upright trace) and compared to that of *p*DFB (inverted trace). It may be seen that in the spectrum of the latter there is very little activity in the low wavenumber (< 300 $cm^{-1}$) spectral range, with just the origin band and the $20_0^2$ overtone band observed; to higher wavenumber are several other vibrations. As well as demonstrating the same vibrational bands, the corresponding spectrum of *p*FT also shows a wealth of weaker bands and, as will be shown, many of these arise from torsions and vibtor levels. We shall discuss the assignment of these bands by the activity we see in the ZEKE spectra recorded via each of the levels in which the REMPI transitions terminate. It will be seen that these assignments are consistent with those that arise by consideration of the 2D-LIF spectra in one of the accompanying papers.[38]

We first note that an electronic-torsion interaction (which can be thought of as a generalized form of the Herzberg-Teller vibronic interaction) allows the $m = 3(+) \leftarrow 0$ torsional transition to be observed in such molecules (see Table II).[44] This has been widely reported and indeed the $m_0^{3(+)}$ transition can be seen clearly here in Figure 2. To confirm, or in a number of cases

ascertain, the assignment of the other bands that appear in the REMPI spectrum, we recorded ZEKE spectra using the different $S_1$ levels as intermediates. In line with other work on such systems, it is expected that the dominant band in the cation will have both the same vibrational and torsional character as the intermediate level (since the geometries and the torsional potentials are expected to be relatively similar). In a generalization of the usual "$\Delta v$ = 0" vibrational propensity rule, we term this a "$\Delta(v,m)$ = 0" propensity rule.

We now move onto presenting the recorded ZEKE spectra, together with comments regarding the resulting assignment of the main features in both the REMPI and ZEKE spectra. The assignment of the intermediate level corresponds to the association of the most intense band in each ZEKE spectrum with the $\Delta(v,m)$ = 0 transition. We denote $S_1 \leftarrow S_0$ transitions in the usual way, noting that we need to specify both the vibrational and torsional level changes. So, for example, we denote the transition from the vibrationless level with one quantum of torsional excitation to the level with one quantum of $D_{20}$ and 4 quanta of torsional excitation as $20_0^1 m_1^4$. We label energy levels with the vibrational label, $D_i$; pure torsional levels with their $m$ number – noting that there are $m$ = 3(+), 3(-) and a corresponding pair of 6(+)/6(-) states; and for vibtor levels we specify both the vibrational and torsional components. Note that for almost all vibrational transitions, we commence from the zero-point vibrational level in $S_1$, while torsional levels can start at $m$ = 0 or 1 (see above). For ZEKE spectra, we will specify the initial $S_1$ level by its $v$ and $m$ quantum numbers, in such cases it is then only necessary to specify the quantum numbers of the resulting cation state, and we show these in a manner consistent with their being the upper levels of a transition. We elect to use this method as some bands appear to arise as a result of small admixtures of other ZOSs, and it becomes cumbersome to include this; hence, the specified initial $S_1$ level may sometimes be such an

admixture, which will be discussed in the text, but not always explicitly noted in the figures. In some cases it is useful to specify the whole $D_0^+ \leftarrow S_1$ ZEKE transition and we then use the same syntax as for the $S_1 \leftarrow S_0$ transition, but with the lower quantum numbers now being those of the $S_1$ state and the higher ones those of the $D_0^+$ state; the context will make it clear to which type of transition we are referring.

**B. ZEKE Spectrum via $S_1$ *m* = 0 and $S_1$ *m* = 1**

With the excitation laser we access the vibrationless-torsionless level of the $S_1$ state via the $0_0^0\, m_0^0$ transition but, as noted above, because of the similarity of the torsional potentials in the $S_0$ and $S_1$ states, we also are accessing the *m* = 1 level of the intermediate $S_1$ state via the $0_0^0\, m_1^1$ transition, which is at almost exactly the same transition wavenumber, recalling that both of the lowest two *m* levels will be populated even under the coldest conditions because of the different nuclear spin symmetries. We then excite out of these levels using the ionization laser allowing us to record ZEKE spectra. The recorded spectrum is very similar to that reported by us in ref. 37, and so we only show a vertically-expanded view of the low-wavenumber region of the new spectrum in Figure 3, with an expanded view of the first 150 $cm^{-1}$ presented in Figure 4(b). All ZEKE spectra have been calibrated to an adiabatic ionization energy of 70946 $cm^{-1}$ corresponding to the origin transition, in line with our earlier value.[37]

Close to the very strong $\Delta v = 0$ origin band, there are a number of significantly weaker bands, with the first of these appearing as a barely-discernible shoulder on the blue edge of the origin band; however, it can be seen more clearly in the ZEKE spectrum recorded via the $S_1$ *m* = 2 level – see below and Figure 4(c). The assignment of the first and third of these features at 17

$cm^{-1}$ and 78 $cm^{-1}$ to $\Delta m$ = 3 transitions terminating in the $m$ = 2 and $m$ = 4 levels of the cation is relatively straightforward; this region is also shown in Figure 4(b). (Note that the $m$ levels are doubly degenerate and signed, hence the first transition is more correctly labelled as $m = \pm 2 \leftarrow \mp 1$.) These two bands appear clearly in the ZEKE spectrum since we still have population in the $m$ = 1 level, as noted above. (It should be noted that here and elsewhere, transitions originating at $m$ = 1 in the $S_0$ state will appear in the REMPI spectrum at a transition wavenumber that is lower than the actual $S_1$ relative wavenumber by the $S_0$ $m$ = 1 – $m$ = 0 spacing; this shift will also be present for such bands in the ZEKE spectra.) The second band at 48 $cm^{-1}$ may be assigned to one of the $m$ = 3 levels, but it is not immediately clear whether this should be to the $m$ = 3(+) or $m$ = 3(-) level and we shall discuss this further below.

To higher wavenumber in Figure 3, we see other bands whose identity will be discussed below, as these are seen when exciting through other intermediate levels which secures their assignment. We shall, however, highlight the bands at 112 $cm^{-1}$ and 271 $cm^{-1}$ which are assigned as arising from the $b_1$ vibrations, $D_{20}$ and $D_{19}$, respectively, and the band at 352 $cm^{-1}$ which is assigned as arising from the $a_2$ vibration, $D_{14}$; these are in excellent agreement with our calculated wavenumbers (Table I). Each of these is FC (symmetry) forbidden and corresponding bands were seen in the corresponding ZEKE spectrum of *p*DFB[54] – we shall discuss their appearance later; additionally, we shall also see that many of the ZEKE spectra show $D_{14}$ and $D_{19}$ in symmetry-forbidden combinations. At 441 $cm^{-1}$ is the intense, symmetry-allowed $D_{11}$ ZEKE band and combination band with this vibration are also present in most spectra. The assignments of these higher-wavenumber features are largely the same as in our previous publication,[37] albeit with a different nomenclature; we shall address this higher-wavenumber region in more detail in a future publication.[55]

**C. ZEKE Spectrum via $S_1$ *m* = 2**

We access the *m* = 2 level in the $S_1$ state via the $0_0^0\, m_1^2$ transition which can be considered as a cold band, owing to the different nuclear spin symmetries of the *m* = 0 and *m* =1 levels; it is a $\Delta m$ = 3 transition – see Figure 4(a). The ZEKE spectrum exciting via this level is presented in Figure 4(c) and it is clear that the origin band is very weak, and there is a single intense band seen at 17 $cm^{-1}$ – this corresponds to the shoulder on the blue edge of the origin band, seen when exciting from the *m* = 0 and *m*= 1 levels – see Figures 3 and 4(b). The 17 $cm^{-1}$ ZEKE band may be assigned as a transition to the *m* = 2 level in the cation, in line with the $\Delta(v,m)$ = 0 propensity rule. The transition may be designated $0_0^0 m_2^2$ and it will appear at a wavenumber that is lower than the actual value relative to the $S_1$ *m* = 0 level by the $S_0$ *m* = 1 – *m* = 0 spacing.

**D. ZEKE Spectrum via $S_1$ 0 *m* = 3(+)**

When we excite at a wavenumber corresponding to the middle of the $0_0^0\, m_0^{3(+)}$ transition, we observe the ZEKE spectrum shown in Figure 4(d). As may be seen, it is dominated by a ZEKE band at 51 $cm^{-1}$. Interestingly, this is not at precisely the same position as the *m* = 3 band observed via the $S_1$ *m* = 0 level and we conclude these are different bands. Since the assignment of the initial $S_1$ level is secure as *m* = 3(+), then the $\Delta(v,m)$ propensity rule suggests that the intense ZEKE band at 51 $cm^{-1}$ corresponds to a transition to the *m* = 3(+) level in the cation and this then implies that the band seen via the origin is in fact the 3(-) band at 48 $cm^{-1}$. Although the widths of these bands means that they would overlap, they will be shown to be

different in the below. Additionally, we also find similar behaviour in the *p*-xylene molecule,[56] but there the *m* = 3(-) band is explicitly seen in the REMPI spectrum, and so we could excite through this intermediate state and confirm assignments consistent with the above.

We did not observe a clear band associated with *m* = 3(-) for *p*FT. (We did try probing further back in the beam to try and see the 3(-) transition in a warmer part of the expansion, and also tried expansions using He as the backing gas; however, the spectra deteriorated owing to increased clustering – future experiments may be carried out to investigate this further.) Given the proximity of the two bands under discussion, we investigated this in detail by recording spectra at slightly different wavenumbers of the excitation profiles of both the $S_1$ $0_0^0$ and $S_1$ $m_0^{3(+)}$ transitions. These spectra are shown in Figure 5, with the excitation positions indicated. Careful examination of these indicates that the profiles are different and, in particular, the band maxima are at different positions, regardless of the excitation wavenumber. We also highlight the fact that when exciting at a wavenumber on the blue side of the band, corresponding to the *m* = 3(+) level, a shoulder appears, which is similar to that present in the ZEKE spectrum of toluene reported by Lu et al.;[18] on the other hand, the spectrum recorded via the centre of the band more closely resembles the *p*FT ZEKE spectrum of Takazawa et al.[36] As a consequence, here and elsewhere, some caution is required in the interpretation of the shape of the ZEKE bands and whether observed shoulders are indications of overlapped features, or are simply due to excitation of different tranches of the rotational levels. This changing rotational envelope was highlighted by Lu et al.[18] in their work on phenylsilane, but focused on bands of *e* symmetry in that work.[57]

In conclusion, we assign the ZEKE band at 48 cm$^{-1}$ seen via the *m* = 0 level as a transition to the *m* = 3(-) level, and the band seen here at 51 cm$^{-1}$ as being a transition to the *m* = 3(+) level.

**E. ZEKE Spectrum via $S_1$ *m* = 4**

We access the *m* = 4 level of the $S_1$ state via the $0_0^0\, m_1^4$ transition, which can be considered as a cold band, corresponding to $\Delta m$ = 3. The spectrum is shown in Figure 4(e) and consists of a weak band at 0 cm$^{-1}$, a strong band $\Delta(v,m)$ = 0 band at 79 cm$^{-1}$ and a further weak band at 114 cm$^{-1}$. The most intense band corresponds to the *m* = 4 level in the cation, and is one of the same bands seen via $S_1$ *m* = 1. The weak band at 0 cm$^{-1}$ may be assigned as a transition to the *m* = 1 level of the cation (and corresponds to $\Delta m$ = -3), but the 114 cm$^{-1}$ band is not associated with any torsional level; below we shall assign this as a transition to the $D_{20}$ *m* = 1 level of the cation. The $D_{20}$ *m* = 1 and *m* = 4 levels can interact in the $S_1$ state, both having symmetry *e*′ (see Table III); interaction in the $D_0^+$ state is also possible.

**F. ZEKE Spectrum via the feature at 100–120 cm$^{-1}$**

We now move onto ZEKE spectra obtained when exciting at positions corresponding to the feature that appears in the REMPI spectrum at $0_0^0$ + 100–120 cm$^{-1}$. This feature is shown in expanded form in Figure 6(a) and is in approximately the correct position for the $m_2^5$ hot band transition; however, we did not notice any significant relative intensity changes of this band when we changed expansion conditions, and so the indications are that this feature is

composed of one or more cold bands. We note that Okuyama et al.[30] and Zhao and Parmenter[31] assigned the whole of this feature to the $m_1^5$ transition, while Zhao[32] also indicated that the $20_0^1$ transition may also contribute to this feature. The resulting ZEKE spectra recorded via different positions, $A_1$, $A_2$ and $A_3$, in the band are given in traces (b)–(d) of Figure 6. These spectra exhibit the same intense band at ~120 cm$^{-1}$, although the maximum moves slightly as the excitation position changes. There are two possible reasons for this shifting maximum; first, it may be attributable to changes in the rotational profile (similar to those discussed above for the *m* = 3(+) and *m* = 3(-) levels – see Figure 5); or secondly, it may be a result of one or more other bands gaining in intensity as the excitation position is changed; of course, it could be a combination of these two effects. In addition, the ZEKE spectrum in trace (c) clearly shows a shoulder growing in on the red side at 112 cm$^{-1}$, which is present in the other two spectra, albeit less intense. This shoulder appears to originate from the same band seen when ionizing from the *m* = 4 level – see Figure 4(e). The wavenumber of the main band of ~120 cm$^{-1}$ is slightly lower than expected for accessing either the $D_{20}$ *m* = 2 or *m* = 5 levels in the cation, which are the most likely assignments for this band. We note that Takazawa *et al*.[36] report a ZEKE spectrum *via* their assigned *m* = 5 level, although the wavenumber of this intermediate level is not given therein, which shows a single dominant peak at 124 cm$^{-1}$, which they then assigned as the *m* = 5 level in the cation in that work. Additionally, we also see a weak band at 17 cm$^{-1}$ in the spectra, which is clearest in Figure 6(c), which is attributable to accessing *m* = 2 in the cation. This level could be accessed through either a $\Delta m$ = -3 transition from the $S_1$ *m* = 5 level, or a $\Delta v$ = -1 transition from the $S_1$ $D_{20}$ *m* = 2 level. To higher wavenumber a weak ZEKE band is observed at ~224 cm$^{-1}$ – this is most visible in Figure 6(c) which may be assigned as a transition to $2D_{20}$ *m* = 1 in the cation. This level is accessible from the $S_1$ $D_{20}$ *m* = 2 level as a $\Delta m$ = -3, $\Delta v$ = +1 transition, or *via* the $S_1$ *m* = 5 level

which would require $\Delta m$ = -6, $\Delta v$ = +2 changes, with the latter expected to be significantly weaker than the former.

In the ZEKE spectra shown in Figures 6(c) and 6(d) it may be seen that a band is also growing in at 131–134 $cm^{-1}$. We gain insight into this by considering the spectrum obtained when tuning the excitation laser to $S_1$ $0_0^0$ + 142 $cm^{-1}$, for this the ZEKE spectrum is shown in Figure 6(e). As may be seen, it consists of two clear bands, one at 134 $cm^{-1}$ and one at 154 $cm^{-1}$; the latter is due to overlap of the rotational envelopes of the REMPI transitions at 142 $cm^{-1}$ and 137 $cm^{-1}$, and will be discussed in the next subsection. The more intense ZEKE band appears to be the same as the one that is appearing as a shoulder in the spectra in Figures 6(c) and 6(d), while the weak shoulder to lower wavenumber can be associated with the ZEKE band at ~ 121 $cm^{-1}$ seen in Figures 6(c) and 6(d). We thus conclude that much of the REMPI feature at ~112 $cm^{-1}$ and the one at 142 $cm^{-1}$, and the ZEKE bands at 120 $cm^{-1}$ and 134 $cm^{-1}$, arise from a strong interaction between the respective $D_{20}$ $m$ = 2 and $m$ = 5 levels. The gradual evolution of the ZEKE spectrum with wavenumber as we move across the range corresponding to the REMPI band at 112 $cm^{-1}$, and particularly the appearance of the 134 $cm^{-1}$ band only when exciting to higher wavenumber, suggest that there could be a rotational dependence of the coupling between these levels. This is supported by the fact that there is no clear evidence for a $m$ = 5 feature (at 134 $cm^{-1}$) when exciting at 105 $cm^{-1}$ (position $A_1$), even though these are each of $e''$ symmetry and there is strong evidence from the 2D-LIF spectra[38,39] that these levels are mixed. These states are more separated in $S_0$ ad therefore less likely to be interacting significantly[38] and so the fact that separate features are seen in dispersed fluorescence is evidence that the ZOSs are interacting in $S_1$ and, by analogy, in $D_0^+$. Deperturbation of these coupled levels shows that the $D_{20}$ $m$ = 2 level lies below that of the

$m$ = 5 level, in both the $S_1$ and $D_0^+$ electronic states;[39] therefore we conclude that the eigenstate which gives rise to the 100–120 $cm^{-1}$ band has greater contribution from the $D_{20}$ $m$ = 2 ZOS, while the 142 $cm^{-1}$ level has greater contribution from $m$ = 5; this will be explored further in Ref. 39.

The 112 $cm^{-1}$ ZEKE band observed particularly in the ZEKE spectrum when exciting at position $A_2$ may be attributed to accessing the $D_{20}$ $m$ = 1 level in the cation. This would be a $\Delta m$ = -3 transition, from the $S_1$ $D_{20}$ $m$ = 2 level; as will be seen to be a common theme, observation of the $\Delta v$ = -1 and $\Delta m$ = -3 bands in a ZEKE spectrum is a fingerprint for the identity of the intermediate $S_1$ vibtor level. However, a weak band is also observed at 77 $cm^{-1}$, most noticeable in trace 6(c), which may be assigned as accessing $m$ = 4 in the cation; although this is possible *via* a $\Delta v$ = -1 and $\Delta m$ = -6 from the $S_1$ $D_{20}$ $m$ = 2 level, this would be expected to be very weak. The occurrence of the $m$ = 4 ZEKE band may be rationalized as a weak interaction between the $D_{20}$ $m$ = 1 and $m$ = 4 levels, in either (or both of) the $S_1$ or $D_0^+$ electronic states, as discussed in the previous section. The calculated wavenumber of 111 $cm^{-1}$ for the $S_1$ $D_{20}$ fundamental is close to the wavenumber (112 $cm^{-1}$) corresponding to positon $A_2$. The dependence on the intermediate wavenumber of the intensity of the $D_{20}$ $m$ = 1 band in the ZEKE spectra is indicative of some contribution from $D_{20}$ $m$ = 1…$m$ = 4 level in the centre of the main REMPI band. We note that the 112 $cm^{-1}$ ZEKE band also appeared when exciting via $m$ = 4 – see Figure 4(e), confirming some interaction between these levels. Further, we note that what looks like the corresponding band seen when exciting via the origin has a relative intensity that suggests it arises from vibronic coupling in a manner commensurate with the appearance of the $D_{19}$ ZEKE band; it will then have both $m$ = 0 and $m$ = 1 contributions. On the other hand the ZEKE band that appears when exciting via $m$ = 4 – Figure 4(e) – is expected to

have activity arising from the $20_1^1 m_1^1$ transition, noting that the $m$ = 4 and $D_{20}$ $m$ = 1 levels are likely mixed to some extent.

Additionally, (not shown) a band is seen at 560 cm$^{-1}$ in the ZEKE spectrum, which may be assigned to the combination $D_{11}D_{20}$ $m$ = 2. Interestingly, these ZEKE spectra will be seen to correspond to the few examples where the combination bands involving the $\Delta(v,m) = 0$ band with $D_{19}$ and $D_{14}$ do not appear, although this could simply be a signal-to-noise issue.

In summary, both the 112 cm$^{-1}$ band and the one at 142 cm$^{-1}$ arise from an interaction between the $D_{20}$ $m$ = 2 and $m$ = 5 levels. Each of these two REMPI bands would then be associated with a transition to one of the two eigenstates formed from the $D_{20}$ $m$ = 2 and $m$ = 5 ZOSs, with the lower wavenumber band arising from an eigenstate dominated by the former, and the upper wavenumber band arising from an eigenstate dominated by the latter. Evidence for a contribution from the $S_1$ $D_{20}$ $m$ = 1 level at ~112 cm$^{-1}$ has also been observed.

### G. Excitation via other $S_1$ levels involving $D_{20}$

In Figure 7(a) we show a REMPI spectrum highlighting other vibtor transitions involving $D_{20}$. We then show the ZEKE spectra obtained when exciting at wavenumbers corresponding to each of these three transitions.

***1. ZEKE spectrum via $D_{20}$ m = 3(-)***

In Figure 7(b) we show the ZEKE spectrum recorded via the $S_1$ level accessed when exciting at 137 $cm^{-1}$. We note that this does not correspond to any pure torsional band and so we consider assignments based on vibtor levels involving the $D_{20}$ vibration, which is the only one low enough in wavenumber to be a viable candidate. The ZEKE spectrum is dominated by a band at 155 $cm^{-1}$, which is also seen via the origin, suggesting that it corresponds to a totally symmetric vibtor level. It is straightforward to assign this as a transition to the $D_{20}$ *m* = 3(-) level, which corresponds to one of the key vibtor levels assigned in the work on toluene by Gascooke et al.[14] Other weaker features in the spectrum are also straightforward to assign and these are given in the figure. We particularly note the band at 45 $cm^{-1}$ is assignable as a $\Delta v$ = -1 transition, $20_1^0 m_{3(-)}^{3(-)}$; and the band at 115 $cm^{-1}$ is assignable to a $\Delta m$ = -3 transition, $20_1^1 m_{3(-)}^{\ 0}$. As will prove to be a general observation, in the ZEKE spectra recorded for a particular vibtor level we almost always see ZEKE bands corresponding to $\Delta v$ = -1 and $\Delta m$ = -3 quantum number changes from the initial $S_1$ vibtor level. (Interestingly, we do not see the corresponding $\Delta v$ = +1 or $\Delta m$ = +3 transitions for vibtor levels.) Additionally, in the present case, the presence of the band at 45 $cm^{-1}$ confirms the assignment of the band observed when exciting via the *m* = 0 level as being *m* = 3(-) rather than *m* = 3(+) – see above.

Interestingly, we also see a ZEKE band corresponding to $2D_{20}$ and two associated vibtor levels, and this could be explained by mixing between the totally symmetric $2D_{20}$ and $D_{20}$ *m* = 3(-) levels in the $S_1$ (or $D_0^+$) state, or simply by Franck-Condon activity. To higher wavenumber there are various combination bands whose terminating level involves the $\Delta(v,\mathrm{m})$ = 0 vibtor

level: the one at 425 cm$^{-1}$ is $D_{19}D_{20}$ $m$ = 3(-), the one at 506 cm$^{-1}$ is $D_{14}D_{20}$ $m$ = 3(-), and the one at 595 cm$^{-1}$ is $D_{11}D_{20}$ $m$ = 3(-). It is notable that the first two of these are not totally symmetric, but also that each of these involves a non-totally symmetric vibration that was seen as a fundamental when exciting via the origin for *p*FT[37] (see also Figure 3) and *p*DFB.[54] Combinations involving the $D_{11}$, $D_{14}$ and $D_{19}$ levels will also be a recurring theme in the ZEKE spectra.

A ZEKE spectrum exciting via the same intermediate state was reported by ourselves previously,[37] but the intermediate state was erroneously assigned as Varsányi mode 11, based on the work by Okuyama et al.[30] In fact there is no unique $D_i$ mode that can be associated with such a Wilson mode (see Table I), as it loses its identity in the *para*-disubstituted benzenes;[40] on wavenumber grounds it might be assigned to $D_{20}$, but this would be symmetry forbidden and does not agree well with the calculated value (a good approximation for the vibrational wavenumber of $D_{20}$ is established in the present work, with a more precise one from the 2D-LIF work[38]). The reassignment of the 137 cm$^{-1}$ band to a vibtor level is much more in line with the new assignments for toluene[14] and also fits in with the assignments of the other ZEKE spectra here. This means the wavenumber associated with this band and also the other assignments in ref. 37 for this ZEKE spectrum should be replaced with those given herein. We note that Zhao[32] had also reassigned this band, which had earlier[35] been referred to as arising from an unknown $X_0^1$ transition, to the same transition as noted herein, namely $20_0^1 m^{3(-)}_0$. The latter assignment was also mentioned in ref. 28 where it was noted as being consistent with calculated vibrational wavenumbers therein; additionally, the assignment is implicit in the value of $D_{20}$ reported by Ju et al. in ref. 58.

Finally, we also see a very weak band at 189 cm$^{-1}$ that can be associated with $m$ = 6(+), which we suggest may be interacting weakly in the $S_1$ state with the $D_{20}$ $m$ = 3(-) state, both being of $a_1'$ symmetry.

### *2. ZEKE Spectrum via $D_{20}$ m = 4*

In Figure 7(c) we show the ZEKE spectrum recorded via the $S_1$ level accessed when exciting at 172 cm$^{-1}$. It may be seen to be dominated by a band at 187 cm$^{-1}$. By comparing with torsional spacings in $S_1$ and the cation and noting the assignment of the previous band, it is straightforward to assign this feature to the $D_{20}$ $m$ = 4 level in the cation, with the corresponding REMPI band being assignable to the $20_0^1\, m_1^4$ transition. The other weaker bands in the spectrum are facile to assign and, consistent with earlier comments, we highlight the appearance of the $\Delta v$ = -1 and $\Delta m$ = -3 transitions, $D_{20_1}{}^0 m_4^4$ and $D_{20_1}{}^1 m_4^1$.

Again, we see a ZEKE band arising from a transition to the $D_{20}$ overtone, which likely comes from mixing between $2D_{20}$ $m$ = 1 and $D_{20}$ $m$ = 4 in the $S_1$ state which are both of $e''$ symmetry. Additionally, there are also the combination bands arising from each of the $D_{11}$, $D_{14}$ and $D_{19}$ vibrations with the main, $\Delta(v,m)$ = 0, feature. Interestingly, we also see a band at 351 cm$^{-1}$, which is at the correct wavenumber for $D_{14}$, but other possibilities are $3D_{20}$ $m$ = 2 or $D_{19}$ $m$ = 4. Each of these is of the correct symmetry ($e''$) to interact in the $S_1$ state, but the latter two would appear to be too distant, energetically. An assignment to $D_{14}$ seems the most likely, but this would have to be a transition to $D_{14}$ $m$ = 1 on symmetry grounds (Table III), and arise as a result of interactions in the $S_1$ (or $D_0^+$) state.

It is interesting to note that the ZEKE band seen here is very close in wavenumber to one of those recorded via the overlapped *m* = 6(+) band, which will be discussed below; however, the intermediate levels are securely assigned and no interaction is expected with this level on symmetry grounds and so this must be coincidental. Hence we disagree with the assignment by Okuyama et al.[30] based upon their dispersed fluorescence spectrum that the 172 $cm^{-1}$ $S_1 \leftarrow S_0$ band involves the *m* = 6(+) level; notably, the derived torsional parameters in that work suggested this assignment may have been problematic. This is discussed further in the accompanying 2D-LIF paper[38] and the one focussing on the vibration-torsion interactions.[39]

We note that this band was also reported in ref. 32, but assigned to a transition to *m* = 6(+) therein; we do not agree with this assignment, as that transition has been assigned to a different band (see below.)

***3. ZEKE Spectrum via $S_1$ $2D_{20}$***

In Figure 7(d) we show the ZEKE spectrum recorded via the $S_1$ level accessed when exciting at 220 $cm^{-1}$, which may be seen to be dominated by a band at 222 $cm^{-1}$. With the previous assignments, an approximate value for the wavenumber of the $D_{20}$ vibration in the cation can be deduced that strongly suggests the ZEKE band arises from a transition to the $D_{20}$ overtone. The very close values of the relative wavenumbers of the REMPI band and the corresponding $\Delta v$ = 0 ZEKE band are in agreement with the calculated vibrational wavenumbers (see Table I). The consequent assignment of the REMPI band as arising from the $20_0^2$ transition is consistent with the observation of such bands attributable to this transition in *p*DFB[54] and toluene.[8] We note that we see some ZEKE bands arising from the various vibtor levels

involving $2D_{20}$ to higher wavenumber; however, the torsional spacings are slightly different to those for the origin and the $D_{20}$ vibtor levels, indicative of the expected changing interactions with vibrational quantum number – this will be discussed more fully in ref. 39. A band at 331 $cm^{-1}$ is most likely attributable to a transition to $3D_{20}$, while the band at 369 $cm^{-1}$ is most likely due to $3D_{20}$ $m$ = 3(-). To the red of the main band a series of bands are clearly seen that are attributable to the $D_{20}$ vibration and associated vibtor levels, again consistent with interactions between the vibtor levels involving $D_{20}$ and those involving $2D_{20}$ (see ref. 39) Finally, at the high-wavenumber end of the spectrum may be seen the now-expected bands that are combinations of the main $\Delta(v,m) = 0$ ZEKE feature with the $D_{11}$, $D_{14}$ and $D_{19}$ vibrations.

Note the band to the red of the main ZEKE band at 189 $cm^{-1}$. This can be assigned to a transition to $D_{20}$ $m$ = 4, which would tie in with the other $D_{20}$ transitions observed, but this is also at the same energy as $m$ = 6(+) – see below – which could arise owing to interaction in the $S_1$ state with $2D_{20}$ $m$ = 0. The appearance and intensity of the band suggests that in fact both contributions may be present. Also of note is that bands attributable to both the $D_{20}$ $m$ = 3(-) vibtor level, as well as $m$ = 3(-) band itself, are present in the spectrum, suggesting interaction in the $S_1$ state between the two $a_1'$ symmetry levels, $2D_{20}$ $m$ = 0 and $D_{20}$ $m$ = 3(-); this is as well as the interaction involving $m$ = 6(+) – mentioned above, and discussed further below. We note, however, that the interactions discussed here must be weak, since there is no obvious splitting of the $2D_{20}$ band, and so the transitions involving $m$ = 0 and $m$ = 1 are still overlapped.

Of note is that Okuyama et al.[30] assigned this band in their LIF spectrum to Varsányi mode $\nu_{15}$, which is a vibration of $b_2$ symmetry, but which really ought to be at a significantly higher

vibrational wavenumber (see ref. 40 and Table I). Taking their assignment to imply the lowest wavenumber mode of $b_2$ symmetry, which would be the $D_{30}$ mode, Table I shows even this is at a significantly higher wavenumber; hence the assignment in ref. 30 is incorrect. This incorrect assignment was also perpetuated in our earlier ZEKE study,[37] and the present assignments supersede those. Zhao and Parmenter,[35] and Zhao[32] give an assignment in agreement with that here, and this is also confirmed in ref. 28.

**H. ZEKE Spectrum via $S_1$ m = 6(+)**

In Figure 8(a) we show an expanded view of the REMPI spectrum close to 200 $cm^{-1}$. In between the two most intense bands, which were discussed in the previous subsection, are three features, two weak and one extremely weak. The lower of these will be seen to be attributable to the *p*FT-Ar complex (see below), with perhaps some contribution from a hot band under some conditions, but the higher wavenumber one at 198 $cm^{-1}$ is due to the *p*FT monomer. When we tune the excitation laser to this wavenumber, we record the ZEKE spectrum presented in Figure 8(b). This shows two bands, one at 188 $cm^{-1}$ and one at 349 $cm^{-1}$. The intermediate level is at the expected position for an $m$ = 6 band, but this could be $m$ = 6(+) or $m$ = 6(-), noting that each of these could shift in wavenumber via interactions with other levels. In addition, we expect the $D_{14}$ vibration to have a wavenumber close to this value, based on the assigned position of the $D_{14}$ overtone band (see below) in the $S_1$ state and additionally the wavenumber of the ZEKE band is in very good agreement with the calculated value for $D_{14}$ in the cation (Table I). (Noting that the $S_1$ $D_{14}$ calculated value is not expected to be reliable, while cation value will be – see comments below.)

We examine the possibilities for the assignment of the 198 cm$^{-1}$ REMPI band. We start by noting that the $D_{14}$ and the $m$ = 6(-) bands have the correct symmetry to interact (see Table III), and so such a narrow REMPI feature is unlikely to arise from an overlap of the $m_0^{6(-)}$ and $14_0^1$ transitions: the two resulting eigenstates would be expected to be separated by significantly more than the width of this feature, but it is not necessary that they interact, of course. We next note that if the $D_{14}$ and $m$ = 6(-) ZOSs are interacting then it is possible that the 198 cm$^{-1}$ REMPI feature could originate from a transition to one of the two resulting eigenstates; this would then require a partner band corresponding to the other eigenstate – see below. A second possibility is that the band arises from an overlap of $m_0^{6(+)}$ and another transition to a level that is one of the eigenstates formed from the $m$ = 6(-) and $D_{14}$ ZOSs, but again requiring a further partner band. Confirmed here, following indications that such a band is present from the 2D-LIF study,[38] a weak band is present at just over 200 cm$^{-1}$ that can be assigned to the other eigenstate; however, given its weakness relative to the other band, the indications are that any such interaction is extremely weak. This is supported by further evidence, to be discussed later, that there is an associated weak interaction between the $D_{14}$ $m$ = 6(-) and 2$D_{14}$ levels, which are the corresponding combination bands (with $D_{14}$) of the features being discussed. We conclude, therefore, that the 198 cm$^{-1}$ REMPI feature arises from an overlap of the $m_0^{6(+)}$ transition and a transition to an eigenstate that is almost entirely composed of the $D_{14}$ ZOS, but with a small contribution from $m$ = 6(-); the corresponding transition for the second eigenstate gives the very weak band just above 200 cm$^{-1}$.

The tentative assignment of Zhao[32] of this band to the $20_0^1 m^{3(+)}_0$ transition does not appear to make sense as this would be at a different wavenumber.

**I. ZEKE spectra via vibtor levels involving $D_{19}$**

In Figure 9(a) we show a portion of the REMPI spectrum of *p*FT, with bands highlighted that involve transitions to levels involving $D_{19}$. We recorded ZEKE spectra via these levels, and these are displayed in the traces presented in Figures 9 (b)–(e). Note that, as with $D_{20}$, we also observe an overtone band, $19_0^2$, in the REMPI spectrum at 484 cm$^{-1}$, and this will be discussed in a subsequent subsection.

***1. ZEKE Spectrum via* $S_1$ $D_{19}$ *m* = 2**

In Figure 9(b) we show the ZEKE spectrum recorded via the $S_1$ level accessed when exciting at 256 cm$^{-1}$, marked as position $B_1$ in Figure 9(a), which may be seen to be dominated by a band at 287 cm$^{-1}$. At these wavenumbers in the cation, we expect contributions from vibtor levels associated with the $D_{19}$ vibration (Table I) and the best assignment for the ZEKE band is to the $D_{19}$ $m$ = 2 cation level, which implies that the corresponding REMPI band arises from the $19_0^1\, m_1^2$ transition. (Note that in ref. 37 this REMPI band was incorrectly assigned as a transition involving solely Varsányi mode 10b, i.e. $D_{19}$.) To lower wavenumber we see the expected $\Delta v$ = -1 band at 17 cm$^{-1}$, corresponding to the $19_1^0 m_2^2$ transition, and we also see a weak feature at 271 cm$^{-1}$ that can be assigned to the $\Delta m$ = -3 transition, $19_1^1 m_2^1$, based upon the good agreement with the calculated value for $D_{19}$ – this assignment is supported by the appearance of a similar band when exciting via the $D_{19}$ $m$= 3(-) level – see below. To higher

wavenumber the bands at 559, 638 and 727 cm$^{-1}$ may be assigned to the combinations of the main $\Delta(v,m) = 0$ feature with $D_{19}$, $D_{14}$ and $D_{11}$.

Of particular interest is the feature that appears at 250 cm$^{-1}$, noting also that the feature at 690 cm$^{-1}$ is consistent with being the combination with $D_{11}$. The assignment of the lower-wavenumber band at 250 cm$^{-1}$ does not fit any other vibtor level involving the $D_{20}$ or $D_{19}$ vibrations and so, owing to the limitations on what this can be, we conclude it is most likely to be the $m = 7$ band, which fits the expected position extremely well in the cation, and the REMPI band is reasonably close to its expected position. Although this could be rationalized as a $\Delta v = -1$, $\Delta m = \mp 9$ ($\mp 7 \leftarrow \pm 2$) transition, which is an allowed change in $m$ that is a multiple of 3, this would be expected to be vanishingly weak. Since the ZEKE band is at the expected position, based on what we see in the ZEKE spectrum, we suggest that the ZEKE feature arises from a transition that conserves the torsional excitation. i.e. $m_7^7$. As such, this suggests that the REMPI band at 256 cm$^{-1}$ is actually an overlapped feature, which its profile does suggest – see expanded view in Figure 9(a) – with the weak $m_1^7$ band underlying the stronger $19_0^1\, m_1^2$ feature. Although these are of the same symmetry (*e*″), it seems that these are only interacting weakly, since they seem to be close; consistent with the large $\Delta m$ required.

Interestingly, exciting at a wavenumber corresponding to a position on the blue side of this this REMPI band, marked $B_2$ in Figure 9(a), we find the 250 cm$^{-1}$ feature is not present – see Figure 9(c), suggesting the $m_1^7$ band (or the band dominated by this transition) is located on the red side of the main REMPI feature; as a consequence, exciting at the peak of the main feature would be exciting higher rotational levels of this overlapping band and hence give the pseudo double-band appearance of the ZEKE band at 250 cm$^{-1}$. The $m = 7$ band in the $S_1$ state

appears to be at a slightly lower wavenumber than expected, and this suggests it is interacting with a higher-wavenumber state of *e*″ symmetry. There are various candidates, with the closest in wavenumber being $D_{19}$ *m* = 4: this level might be expected to interact more strongly than $D_{19}$ *m* = 2, which is also of *e*″ symmetry, because of the decrease in strength of coupling with increasing difference in *m* quantum number between two interacting states (however, it is also energetically more distant and so a fuller consideration of the interactions is required). This could tie in with the appearance of the weak $D_{19}$ *m* = 4 band at 348 $cm^{-1}$, and the associated *m* = 4 band at 78 $cm^{-1}$; alternatively, the latter band could appear from a $\Delta m$ = -3 transition from *m* = 7.

Interestingly, Okuyama et al.,[30] Zhao and Parmenter,[31] and Zhao[32] assigned a corresponding band in their LIF spectrum to the $m_1^7$ transition. The dispersed fluorescence spectrum in ref. 30 is unusual in that the expected $\Delta(v,m)$ = 0 band is not the most intense; this behaviour would be much more in line with this band being an overlapped feature as suggested here and in the accompanying papers.[38,39] The disagreement with calculated line position in the $S_1$ state (but good agreement in the $S_0$ state), based upon derived torsional parameters, is noteworthy and, as will be seen in the accompanying papers,[38,39] is evidence that torsion-vibrational coupling is occurring. Zhao[32] did suggest that this band may be overlapped with another feature, but suggested this was $19_0^1$ – as noted above we do not agree with this assignment.

### *2. ZEKE Spectrum via $D_{19}$ m = 3(-)*

In Figure 9(d) we show the ZEKE spectrum recorded via the $S_1$ level accessed when exciting at 283 cm$^{-1}$, which may be seen to be dominated by a band at 319 cm$^{-1}$. With knowledge of the assignment of the $D_{19}$ $m$ = 2 band, the main ZEKE band can be assigned as a transition to $D_{19}$ $m$ = 3(-), and so the REMPI transition is assigned as $19_0^1 m^{3(-)}_0$. Again, we see the main feature in combination with the $D_{11}$ and $D_{19}$ vibrations, with a very weak transition to the $D_{14}$ combination also being observed. In line with the spectra discussed above, we also see the $\Delta m$ = -3 and $\Delta v$ = -1 bands to lower wavenumber, these correspond to the $19_1^1 m_{3(-)}^0$ and $19_1^0 m_{3(-)}^{3(-)}$ transitions, respectively. There are several other bands that require assignment at 189, 384, 427, 462 and 490 cm$^{-1}$. The 189 cm$^{-1}$ band is the $m$ = 6(+) band, and again suggests interaction between various totally symmetric levels in $S_1$; the 462 cm$^{-1}$ band can then be associated with $D_{19}$ $m$ = 6(+). (Note that the 189 cm$^{-1}$ ZEKE band is not associated with $D_{20}$ $m$ = 4, since it would need to originate at $m$ = 1; additionally, we see no other evidence of interactions between vibtor levels separately involving $D_{19}$ and $D_{20}$.) The band at 384 cm$^{-1}$ matches extremely well the expected position for the $D_{19}D_{20}$ combination band, which is confirmed by a weak ZEKE spectrum recorded via a level at $S_1$ $0_0^0$ + 353 cm$^{-1}$ (see later); this then suggests an assignment of the 427 cm$^{-1}$ ZEKE band as a transition to $D_{19}D_{20}$ $m$ = 3(-) and the 490 cm$^{-1}$ band to the ($D_{19}$ + 2$D_{20}$) combination.

This REMPI band appears to have been incorrectly assigned to the $v_{11}$ overtone (Varsányi nomenclature) by Okuyama et al.[30] In earlier work, Zhao and Parmenter[35] merely designated

this band as arising from a $X_0^2$ transition, but then Zhao[32] later assigned this band to the same transition as we conclude here.

### *3. ZEKE Spectrum via $D_{19}$ m = 4*

The final vibtor level involving the $D_{19}$ vibration gives rise to a very weak band found at 320 cm$^{-1}$, and the corresponding ZEKE spectrum – see Figure 19(e) demonstrates a $\Delta(v,m) = 0$ band at 350 cm$^{-1}$, which ties in with its being the $D_{19}$ $m$ = 4 level, and so the REMPI band is $19_0^1 m_1^4$. Thus, the same complement of vibtor levels involving $D_{19}$ is seen as was the case for $D_{20}$. Zhao[32] tentatively suggested that this band may be due to the $20_0^3$ transition, but we do not concur with this suggestion.

## J. $D_{30}$, "Ripples" and *p*FT-Ar and *p*FT-Ar$_2$ Bands

In Figure 10(a) we show a close-up of the REMPI spectrum recorded in the *p*FT mass channel in the range 300–420 cm$^{-1}$ (to appreciate the weakness of these features, the reader should look back to this region in Figure 2(a)). This region consists of a band at 311 cm$^{-1}$, plus a series of "ripples" leading up to the pair of bands at 400–420 cm$^{-1}$ – the latter will be discussed in more detail below. There are various possible contributions here, and the assignment of these and associated ZEKE spectra, is based on a number of points: (i) we expect the $D_{30}$, $D_{14}D_{20}$ and $D_{19}D_{20}$ bands to appear in this region and additionally there can be vibtor levels associated with these; (ii) most of these bands are very weak and consequently hot bands associated with the Fermi resonance bands at 400–420 cm$^{-1}$ need to be considered; (iii) bands associated with dissociation of *p*FT-Ar and *p*FT-Ar$_2$ complexes could appear in this region of the *p*FT REMPI spectrum.

To test the latter we recorded mass-resolved REMPI spectra using two-colour ionization, in order to minimize the extent of fragmentation, gating the ions of each of *p*FT-Ar and *p*FT-$Ar_2$. The spectra are shown in Figure 11 along with that of *p*FT itself. As may be seen there are matches for three bands in the 300–390 $cm^{-1}$ region for *p*FT-Ar and for two from *p*FT-$Ar_2$, hence bands in the *p*FT mass channel at these positions are largely due to the complexes. Although hot bands may also be expected at these wavenumbers, the indications are that these contributions are small, with the most likely ones being those of the bands marked as *p*FT-$Ar_2$ at 330–340 $cm^{-1}$, since there is no band in the *p*FT channel that corresponds to the origin (see Figure 11); either way, these bands do not seem to be due to cold *p*FT. It is also of note that a weak band at 188 $cm^{-1}$ seems to be associated with the *p*FT-Ar complex. Some of the features associated with the complexes did give rise to ZEKE bands, but their assignment is currently unclear and pending a more detailed examination of ZEKE spectra for these species.

We now examine the cases where ZEKE spectra attributable to *p*FT could be recorded at positions across this region, recalling that we have already assigned the REMPI band at 320 $cm^{-1}$ as being attributable to the $19_0^1 m_1^4$ transition. In Figures 10(b) – (d) we show ZEKE spectra recorded when exciting at three different positions within the band at 311 $cm^{-1}$, which are labelled $C_1$, $C_2$ and $C_3$ in Figure 10(a); these each show three ZEKE bands over the range scanned. The ZEKE band at 321 $cm^{-1}$ may be confidently assigned as a transition to the $D_{30}$ cation vibration, on the basis of the calculated vibrational wavenumber (see Table I), with the band at 763 $cm^{-1}$ then being $D_{11}D_{30}$. (It is interesting to note that for this non-totally-symmetric vibration, the combination bands involving $D_{14}$ and $D_{19}$ did not appear, but this could simply be a signal-to-noise issue.) The band at 463 $cm^{-1}$ may be assigned to the $D_{14}D_{20}$

combination band, based on values for the individual vibrations in both the $S_1$ state and the cation. No ZEKE spectra recorded at other positions gave rise to the $D_{30}$ and $D_{14}D_{20}$ features. We conclude that the REMPI band at 311 cm$^{-1}$ is largely composed of two overlapped bands corresponding to the transitions $30_0^1$ and $14_0^1 20_0^1$ and that, even though the terminating levels each have $b_2$ symmetry, there appears to be no significant interaction between them.

We note that Okuyama et al.[30] and Zhao and Parmenter[32] assigned this band to the $m_1^8$ transition, so presumably as a result of a $\Delta m$ = 9 transition ($m$ = 8 ← $m$ = -1), but we would expect this to be extremely weak, and so reject this assignment. The evidence from the ZEKE spectra, combined with the calculated wavenumbers and those already derived from other REMPI and ZEKE spectra above, supports the present assignment. Zhao and Parmenter[35] and Zhao[32] suggest that the band is an overlap of two features, but of the $30_0^1$ with the $m_1^8$ transition; we only concur with the former assignment.

The two spectra recorded on the low wavenumber side of the band, at position $C_1$ and $C_2$, are surprisingly similar – see Figures 10(b) and 10(c). However, when exciting at higher wavenumber, at position $C_3$, we see a further ZEKE feature at 300 cm$^{-1}$ – see Figure 10(d). Based on the $S_1$ and $D_0^+$ wavenumbers, a reasonable assignment for this latter band is to one of $D_{20}$ $m$ = 6(-) or $D_{20}$ $m$ = 6(+). The $D_{20}$ $m$ = 6(-) has symmetry $a_1''$, which allows it to gain intensity via vibronic coupling and/or interact with the $D_{30}$ $m$ = 0 vibrational state and so gain intensity from it (but the interaction must be relatively weak as these bands are very close); on the other hand there are no obvious mechanism by which the $D_{20}$ $m$ = 6(+) level can gain intensity, and so the former assignment is favoured.

Assignments of the other bands in this region can be deduced as the following based on their $S_1$ and $D_0^+$ wavenumbers (note that these spectra were very weak and so mostly only a $\Delta(v,m)$ = 0 band was observed in each ZEKE spectrum; some of these spectra are not shown). As mentioned above, the REMPI band at 320 cm$^{-1}$ shows a $\Delta(v,m)$ = 0 band at 350 cm$^{-1}$ and the REMPI band is $19_0^1 m_1^4$. No ZEKE spectrum could be recorded for the REMPI band at 323 cm$^{-1}$ band owing to its weakness, but the REMPI band is in the correct position to be $30_0^1 m_1^2$. The REMPI band at 353 cm$^{-1}$ gave rise to a $\Delta(v,m)$ = 0 ZEKE band at 382 cm$^{-1}$, and this ties in with the REMPI band being $19_0^1 20_0^1$; this band has appeared in other ZEKE spectra at about the same position. (This REMPI band may be the same as an unassigned band at 351 cm$^{-1}$ noted by Zhao.[32])

The feature at 360-367 cm$^{-1}$, marked D in Figure 10(a), appears to consist of three contributions. The blue edge is one of the *p*FT-Ar bands commented on in the above. When exciting at 361 cm$^{-1}$ (on the red side of feature D) we obtain a ZEKE spectrum (not shown) with a $\Delta(v,m)$ = 0 ZEKE band at 368 cm$^{-1}$, and we tentatively assign this as a transition to the $D_{30}$ $m$ = 3(+) level, which is totally symmetric ($a_1'$) overall (see Table III); this assigns the transition of $30_0^1 m^{3(+)}_0$ to a REMPI band at this position. When exciting at the position of the centre of the band, at 364 cm$^{-1}$, we obtain the ZEKE spectrum shown in Figure 10(e), with the strongest band at 536 cm$^{-1}$. This band appears to be the same as that observed when exciting within the band at 400 cm$^{-1}$ (see below). We deduce the assignment of the ZEKE band to be a transition to the $D_{14}$ $m$ = 6(-) level which is an overall totally symmetric ($a_1'$) vibtor level, with the involvement of $D_{14}$ confirmed by the very large shift in the relative wavenumber of the $\Delta(v,m)$ = 0 ZEKE band compared to that of the corresponding REMPI band. We shall refer back to this ZEKE band later.

Interestingly, Zhao[32] noted that this feature may contain four contributions, with the suggestions being $30_0^1 m^{3(+)}_0$,$14_0^1 m^{6(-)}_0$, $19_0^1 20_0^1$ and (tentatively) $17_0^1$ as discussed above. We concur with the first two assignments, but not with the latter two: we have assigned the $19_0^1 20_0^1$ transition to a band at 354 cm$^{-1}$, and we expect $D_{17}$ to have a wavenumber of ~537 cm$^{-1}$ in the $S_1$ state (Table I).

**K. ZEKE Spectra when Exciting Across the 395–415 cm$^{-1}$ Range**

In Figure 12, we show a close-up of the REMPI spectrum across the range 395–415 cm$^{-1}$ as a vertical trace on the right-hand side, which consists of two main features, E and F. These two features were studied in our previous paper[37] where the second feature (F) was concluded to be almost exclusively associated with the $11_0^1$ transition, and the first feature (E) was concluded to be two overlapped bands: $14_0^2$ and $29_0^1$ (although Varsányi labels were used in that work). Here, we record a series of ZEKE spectra while stepping the excitation laser across this region, yielding what we term a 2D-ZEKE spectrum, and this is also shown as the main part of Figure 12. Each separate ZEKE spectrum is identified by a label and is linked to the position on the REMPI spectrum at which excitation occurred by a dashed line. Starting at the higher wavenumber end (feature F), we see that the ZEKE spectra are dominated by the $11_0^1$, $\Delta v$ = 0, band together with the pair of $\Delta v$ = ± 1 bands – the origin (via the $11_1^0$ transition) and $11_1^2$. In addition, a weak band appears at 823 cm$^{-1}$, which is most likely attributable to the FC-allowed $D_9$, based on the calculated wavenumber (Table I). Exciting at three positions ($F_1$–$F_3$) in this band gives essentially the same features, as may be seen from Figure 12. In particular, we note that there is only the faintest trace of a band corresponding to the $14^2$ transition, suggesting at most very little interaction between these two features.

Things are less straightforward when exciting across feature E, and six ZEKE spectra are shown corresponding to excitation positions labelled $E_1$ – $E_6$. It is clear that the largest contributions are from $D_{29}$ when exciting at higher wavenumber, and the $D_{14}$ overtone when exciting to lower wavenumber; this is in accord with the ZEKE spectra reported in ref. 37. However, here we wish to comment on other aspects of these ZEKE spectra. First, the feature at ~540 $cm^{-1}$ may be seen to be due to two close and partially overlapped bands – this is emphasised in Figure 13. In ref. 37 the assignment was to the overtone of Varsányi mode 10*b*, which here we designate $2D_{19}$, and this seems to be a FC-active band associated with ionizing via $2D_{14}$. (This latter assignment is confirmed as described in the following subsection.) The overlapped band at the lower wavenumber, 537 $cm^{-1}$, is the same feature we saw when exciting at 364 $cm^{-1}$ – see above, and Figure 10(e) – and was discussed above; the assignment of this ZEKE band was to an eigenstate with a predominant contribution from $D_{14}\,m$ = 6(-) – Figure 13 compares these spectra in more detail. Hence, we conclude that the appearance of the ZEKE spectra suggests a very weak interaction between the $2D_{14}$ and $D_{14}\,m$ = 6(-) states, both being totally symmetric ($a_1'$).

The band at 364 $cm^{-1}$, discussed above, seems to be largely due to $D_{14}\,m$ = 6(-), with only a small amount of $2D_{14}$; indeed, we could not see a ZEKE feature at the correct position for this, owing to the weakness of the transition – on the other hand we can see the $D_{14}\,m$ = 6(-) band when exciting at the wavenumber of the intense $14^2$ transition. On the other hand, the band in the "Fermi resonance" arises from a level that is very largely $2D_{14}$ with just a small amount of $D_{14}\,m$ = 6(-). It is plausible that the interaction may be stronger, but being affected by

depopulation/dissipative IVR processes – further insight from time-resolved experiments would be extremely useful to provide further insight on this point.

When exciting at a wavenumber corresponding to a dominant $14_0^2$ transition, a ZEKE band that is attributable to excitation of $D_{11}$ is seen; similarly, a weak $14^2$ ZEKE band is seen when exciting at positions $F_1$–$F_3$. (Part of the reason for the extremely weak $14^2$ ZEKE band when exciting via the $D_{11}$ $S_1$ intermediate state could be that the photoionization cross section is larger for $D_{11}$ than for $2D_{14}$.) Overall, there is thus some evidence for a weak interaction between the $2D_{14}$ and $D_{11}$ levels, but it is difficult to be sure that this is not just FC activity; again, time-resolved experiments would be insightful here.

We also note that other weak bands appear that are more pronounced in the ZEKE spectra recorded on the low wavenumber side of the 400 $cm^{-1}$ band. First, we see the $D_{14}$ band whose intensity seems to be linked to that of the $14^2$ band. Also, when exciting to the red edge of the 400 $cm^{-1}$ REMPI band, we see a broadish feature with a maximum at ~402 $cm^{-1}$. Our best suggestion for this is the $2D_{20}$ $m$ = 6(+) band (totally symmetric, $a_1'$), which is likely interacting with $2D_{14}$.

**L. ZEKE Spectrum when exciting via $2D_{19}$**

We recorded a ZEKE spectrum with the excitation laser tuned to 484 $cm^{-1}$ which is where we expect the $19_0^2$ $S_1 \leftarrow S_0$ transition to be. Indeed, we see a strong $\Delta v$ = 0 band, see Figure 13(d), at 542 $cm^{-1}$, which corresponds to the higher wavenumber overlapped band shown in Figure 12 and discussed in the previous subsection, confirming the contribution from this

feature. This is in good agreement with the calculated vibrational wavenumbers in both states (Table I). Note that this band is clearly separate from the band at 537 $cm^{-1}$ that we have assigned as mainly associated with $D_{14}$ $m$ = 6(-) – see previous subsection. The assignment of this REMPI band is in line with that from Zhao and Parmenter[35] and Zhao.[32]

## VI. ADDITIONAL DISCUSSION

### A. Appearance of the $D_{14}$ and $D_{19}$ Bands and their Combinations in the ZEKE Spectra

Various mechanisms for the appearance of the symmetry-forbidden bands, $D_{19}$ and $D_{14}$ in the ZEKE spectrum of *p*DFB have been noted and discussed,[54] although no firm conclusion could be reached as to the actual mechanism involved. We briefly examine the symmetry arguments below in relation to *p*FT.

The ground electronic state of the benzene cation is $^2E_{1g}$ and in $C_{2v}$ this would correlate to $^2B_1$ and $^2A_2$ states (see Figure 1), with the former being the lower and so the ground state. The $D_{19}$ vibration is of $b_1$ symmetry and so a breakdown of the separability of electronic and vibrational motions would lead to vibronic interaction within the ground cationic state. This then would lead to a combined (point group) vibronic symmetry of $A_1$ overall and so provide a vibronic mechanism for the observation of $D_{19}$ and, in a corresponding way, for the various combinations involving this vibration. Of note is that the same mechanism could explain the observation of the $m$ = 3(-) transition – see below.

The $D_{14}$ band is of $a_2$ symmetry, i.e. the same as the first excited cation state, $D_1^+$; however, it is not clear what coupling would lead to this being allowed, since vibronic interaction with the $D_0^+$ electronic state would lead to an overall vibronic symmetry there of $B_2$ symmetry, and there is no clear way by which this could lead to intensity stealing occurring. Another possibility is that there is a distortion of the force field of the $S_1$ state close to the minimum. There is evidence that obtaining reliable $M_{14}$ vibrational wavenumbers for monohalobenzenes is "challenging",[59,60,61] and this could be due to a vibronic or another state-mixing effect being present along this coordinate. The result of that could be a lowering of the symmetry of the observed geometry along that coordinate or, if the effect is small enough, it may merely mean that there is only some distortion of the force field along this coordinate. As discussed in ref. 54, the $D_{14}$ vibration (designated $\nu_8$ in that work) was calculated to be imaginary; however, various papers discussed in that work and subsequently have reported conflicting conclusions as to the geometry of the $S_1$ state of *p*DFB, and this may suggest that the extent of the distortion of the force field can affect the results of some experiments but not others. Additionally, different extents of distortion could be obtained via quantum chemical methods using different levels of theory/basis sets. Such a distortion, combined with the large change in the $M_{14}/D_{14}$ vibrational wavenumber between the $S_1$ and $D_0^+$ states, could be the source of activity of this vibration in the ZEKE spectra.

Also discussed in ref. 54 and elsewhere, although one may discuss the fact that these experiments are ZEKE-PFI experiments, and so access high-lying Rydberg states, the role of the Rydberg electron is unclear, as it is expected to be at large separation from the cationic core and, further, low-$l$ and low-$m_l$ levels are expected to mix and only higher angular

momentum states should survive – these should be poorly penetrating. Overall, therefore, it is not clear how such symmetry arguments could be affecting vibrational activity via vibronic coupling effects.

**B. Torsions, Vibration-Torsion Coupling and the *m* = 3(+)/3(-) Bands**

The appearance of the torsional/vibtor features in the case of toluene has been discussed in detail by Walker et al.[44] and more recently by Virgo et al.[45] with a particular emphasis on explaining the relative intensities of the forbidden bands via the dependence of the $S_1$–$S_0$ transition dipole moment on the torsional angle via a Fourier expansion of the dipole moment in terms of the torsional angle, $\alpha$. As noted above, it was deduced that the $m_0^{3(+)}$ transitions should be the most intense, but that other $\Delta m$ = 3 transitions should be seen, explaining the presence of the $m_1^2$ and $m_1^4$ bands (noting that *m* can be signed).[44] This mechanism may be thought of as a generalized form of a Herzberg-Teller interaction between electronic-torsional levels arising from the $S_1(\tilde{A}\,^2A_1'')$ electronic state and its *m* = 3(+), $a_1''$ symmetry, torsional levels (giving $A_1'$ electronic-torsional symmetry overall) and $A_1'$ electronic-torsional states which could involve either the *m* = 0 torsion of the $S_0$ ($\tilde{X}\,^1A'$), or of the excited $A_1'$ electronic state that occurs as one of the components of the $\tilde{C}^1E_{1u}$ state of benzene (the state that is responsible for the classic vibronic Herzberg-Teller interaction in benzene). The above considerations do not, however, explain the appearance of the very weak $m_0^{3(-)}$ transition, which was suggested as arising from torsion-rotation coupling,[44] with this considered in more detail by Virgo et al.,[45] where simulations gave close-to-quantitative agreement with

experiment, and revealed the dependence of the intensity of the $m_0^{3(-)}$ feature on the magnitude of $V_6$ and the rotational temperature.

The assignments of the features in the REMPI spectra of the $S_1 \leftarrow S_0$ transition in toluene were confirmed by ZEKE experiments[18] based upon expected selection rules and the $\Delta(v,m) = 0$ analogue of the vibrational "$\Delta v = 0$" propensity rule for excitation of the same torsional character in the cation as in the intermediate $S_1$ level. In ref. 14, Gascooke et al. showed that essentially the same assignment resulted when considering vibration-torsion coupled levels, but that the values of the effective rotational constants and $V_6$ barrier height were different – very starkly so for $V_6$. In the absence of any significant perturbation of the potential by the presence of the fluorine atom in *p*FT, we would expect both the appearance of the REMPI spectra for these molecules in this region, and the assignments of the bands, to be similar. This has been confirmed in passing in the above, but will be considered in more detail in an accompanying paper.[39] At this point, we consider in more depth the assignment of the *m* = 3(+) and *m* = 3(-) levels.

***1*. *m* = 3(+) and *m* = 3(-)**

As noted above, we observed two bands in the spectral region corresponding to the expected position of m = 3, at 48 and 51 $cm^{-1}$, with the lower wavenumber band appearing when exciting via the $S_1$ *m* = 0 level, and the upper wavenumber band appearing when exciting via the $S_1$ *m* = 3(+) level. The $\Delta(v,m) = 0$ propensity rule, which appears to work well for all examined ZEKE transitions here, therefore strongly points to the higher level in the cation being assigned as *m* = 3(+). This then must mean that *m* = 3(-) is the lower level in the cation,

which is the level observed when exciting via the $S_1$ $m$ = 0 level. We emphasise that these two levels are quite close, and so difficult to separate definitively using ZEKE spectroscopy, but the ZEKE spectra, shown in Figure 5 and discussed above, strongly suggest that this proposed assignment is correct. (This assignment is also in concurrence with a similar assignment in *p*Xyl,[56] as we mentioned above.) We now discuss the assignments of these levels in *p*FT and toluene, as well as other molecules. First, we note that the ZEKE spectra of Takazawa et al.[36] only have a quality sufficient to observe the "$\Delta m$ = 0" torsional band in each case and hence no information on other torsional levels is available from that work; in addition, they appear to have used the assignments of Okuyama et al.[30] which are not all correct (see above). As such, their derived torsional parameters may be in error – in any case the value of $V_6$ (-33.7 $cm^{-1}$) depended on the position of the $m$ = 3(+) band in the absence of observation of the $m$ = 3(-) band, and also any vibration-torsion interactions were neglected. Further, in an endnote (#20) to their paper on torsional band intensities, Walker et al.[44] comment that they had recorded spectra with improved signal to noise and deduced the value of $V_6$ to be $\leq$ 5 $cm^{-1}$, although the sign could not be determined; since this spectrum has never been published, as far as we have been able to ascertain, it is unclear whether both $m$ = 3 states were observed or what other assignments they made different to those in refs. 30 and 36.

We may, however, compare to the ZEKE study of Lu et al.[18] on toluene. In that work ZEKE spectra were recorded via the $m$ = 0 and $m$ = 3(+) levels. In the former case, a band at 45 $cm^{-1}$ was observed, while in the latter case a band at 47 $cm^{-1}$ was observed; in addition, when exciting via $m$ = 3(+), a shoulder appeared on the blue side of the band at 54 $cm^{-1}$. From these results, it was concluded in ref. 18 that the 45 and 47 $cm^{-1}$ bands were the same, and assigned as arising from a transition to $m$ = 3(+) in the cation, from both intermediate levels, and that

the 54 $cm^{-1}$ shoulder was due to $m$ = 3(-). Regarding this shoulder, we note that in a MATI study on toluene, Gunzer and Grotemeyer[19] recorded a spectrum via the $m$ = 0 and $m$ = 3(+) levels (although the band associated with the latter was simply denoted as a generic torsion in that work and it was noted that the assignment was unknown, even though this had been reported in ref. 18): no such shoulder is visible in their spectrum. Further, in the present case of *p*FT we were able to record spectra both with and without a shoulder, depending on where in the band we excited (see Figure 5). The shoulder appears to be simply an artefact of the different subsets of (full molecular) rotational levels associated with the position at which excitation occurs. We hence conclude that the shoulder in ref. 18 is an artefact and that in toluene the $m$ = 3(-) band lies at 45 $cm^{-1}$ and the $m$ = 3(+) band lies slightly higher at 47 $cm^{-1}$. We also note that MATI bands in slightly different positions were observed in ref. 19, consistent with our revised conclusions regarding ref. 18 and the present results on *p*FT.

It is of note that in a study on phenylsilane[57] there was an intense ZEKE band arising from excitation of $m$ = 3(+) observed when exciting via the origin of phenylsilane (but also a 3(-) band was observed); and additionally, there was also a very strong band following excitation via $D_{29}$. These are both of $a_1''$ symmetry and so the explanation for their appearance was based on the presence of the low-energy $D_1^+$ cation state, which is a $^2A_2'$ state, while the $D_0^+$ state is $^2A_2''$, and since $a_1'' \times A_2'' = A_2'$, these may vibronically couple. We also note the appearance of a strong $m$ = 3(+) band in the ZEKE spectrum of 2,6-difluorotoluene (2,6-dFT) also recorded by Weisshaar's group[62] although the spectrum did not extend high enough in wavenumber to include the expected position of the $D_{29}$ band. In the present work, we see a weak $D_{29}$ band via the origin (which appears as a shoulder on the stronger $D_{11}$ band – see Figure 3), which we hypothesise is also due to a vibronic interaction with the higher-lying $D_1^+$

state. If this lies significantly higher in wavenumber than the corresponding state in phenylsilane or 2,6-dFT, then this would be an explanation as to why we do not see the *m* = 3(+) band in the case of *p*FT when exciting via the origin. We suggest that there are two mechanisms for the appearance of the *m* = 3(-) band: vibronic coupling within the $D_0^+$ state, which is present for all substituted benzenes studied; and rotation-torsion coupling which gives additional intensity to this band on occasions when the 3(+) band appears by virtue of the inter-state vibronic coupling. We also note that no $D_{29}$ band (denoted $\nu_{27}$ in $D_{2h}$ Mulliken notation therein) was seen in the ZEKE spectrum of *p*DFB by Reiser et al.,[54] suggesting that its appearance is indeed molecule-specific and, we suggest, dependent on the relative positions of the $D_0^+$ and $D_1^+$ states. With the conclusion above, that the band seen by Lu et al.[18] when exciting via the origin of toluene is actually the *m*= 3(-) band, then this feature is seen in toluene, *p*FT, phenylsilane and 2,6-dFT. The suggested vibronic coupling of the *m* = 3(-) state within the $D_0^+$ state is analogous to the appearance of the *m* = 3(+) band in the $S_1 \leftarrow S_0$ transition, which is a vibronically-allowed $A_1' \leftarrow A_1'$ transition, as discussed by Walker et al.[44]

The above results mean that the *m* = 3(-) state lies below the *m* = 3(+) one, and hence that we expect the $V_6$ parameter to be negative, based upon the separation of the two *m* = 3 torsional levels. However, the value is going to be small and hence it is possible that appropriate inclusion of vibration-torsional interactions could change the value and even the sign of this parameter and, further, that deductions regarding eclipsed/staggered geometries may turn out to be erroneous[16] and hence some caution is required here. Further consideration of the various interactions is presented in a forthcoming paper.[39]

**2. $2D_{14}...D_{11}...D_{14}$ *m* = 6(-) and $2D_{19}$**

We have discussed the appearance of the 395-415 cm$^{-1}$ region of the REMPI spectrum in detail above, together with links to a band that appears at 364 cm$^{-1}$ and another that appears at 484 cm$^{-1}$. When exciting via the levels that give rise to these two latter REMPI bands, ZEKE bands arise that are also seen when exciting across the 395-415 cm$^{-1}$ range – see discussion above and Figures 12 and 13. First, we note that it is clear that the band at ~402 cm$^{-1}$ arises from the $D_{29}$ fundamental and another eigenstate that is predominantly composed of the $D_{14}$ overtone, while the ~411 cm$^{-1}$ band arises from an eigenstate that is predominantly the $D_{11}$ fundamental. It is also clear that there are two bands in the ZEKE spectrum at ~535–545 cm$^{-1}$, whose relative intensities are difficult to disentangle, although both seem to appear when the ZEKE band assigned to $2D_{14}$ is the most intense; we have assigned these two ZEKE bands as arising from excitation of $D_{14}$ *m*= 6(-) and $2D_{19}$. In Figure 13 we show these various transitions in more detail. We first note that REMPI bands attributable to $19_0^2$ have been seen in the spectra of other substituted benzenes, such as *p*DFB (see Figure 2). Also, this band appears to higher wavenumber than the $11_0^1$ transition, even though it appears more intensely when the (lower wavenumber) $14_0^2$ band is the more intense – i.e. the $D_{19}$ overtone activity appears to be associated more with that of the $D_{14}$ overtone than with $D_{11}$. Overall, we conclude that the $D_{19}$ overtone transition is inherently bright in the $S_1 \leftarrow S_0$ transition The accompanying band, assigned to the $14_0^1 m_0^{6(-)}$ transition, could be attributed to Fermi resonance (with $2D_{19}$) in the cation, as these bands are so close to each other; however, we note that we saw a band at 536 cm$^{-1}$ when exciting at 364 cm$^{-1}$ – see Figure 13(b) –, suggesting that the REMPI band arises from a component of a weak Fermi resonance of the $D_{14}$ *m* = 6(-) with the $D_{14}$ overtone. Since we see no evidence of a band for $D_{14}$ *m* = 6(-) when exciting via the $19_0^2$ transition and

vice versa, FR between these two levels seems unlikely. We emphasise that the $14_0^1 m_0^{6(-)} \ldots 2D_{14}$ interaction seems to be very weak from the relative intensities of the bands in Figure 12, and this would also explain the absence of the $2D_{14}$ band in Figure 13, as essentially only the $\Delta(v,m) = 0$ band is seen. These conclusions are all based on evidence occurring on the timescale (ns) of the present experiments.

We reach a similar conclusion when considering whether the $D_{11}$ and $2D_{14}$ levels are in Fermi resonance. Certainly we see a weak $D_{11}$ ZEKE band when exciting via portions of band E, and a very weak $2D_{14}$ band when exciting via portions of the band F (see Figure 12); but, we are unable to be sure whether this is just a reflection of FC activity or a true indication that the associated levels are in Fermi resonance.

***3. $D_{14}D_{20}$* and *$D_{30}$***

As discussed above, we conclude that the $D_{30}$ and $D_{14}D_{20}$ bands have almost coincident wavenumbers and so appear essentially completely overlapped in the REMPI spectrum at ~310 cm$^{-1}$. This is interesting, since these are both of $b_2$ symmetry and so may be thought to interact. We note that in the REMPI spectra of chlorobenzene[60] and bromobenzene[61] bands attributable to both of these equivalent vibrations appear, but do seem to be energetically separate from each other, particularly in the case of chlorobenzene; moreover, in fluorobenzene[59] only the equivalent of the $D_{30}$ band appears in the REMPI spectrum. Further, in the LIF spectrum of *p*DFB[22], the $D_{14}D_{20}$ band appears, but the $D_{30}$ one does not – this may be rationalized since, under $D_{2h}$ point group symmetry, the combination band is of $b_{3g}$ overall, and so is HT-allowed, while the $D_{30}$ vibration is $b_{2u}$ and so forbidden. We conclude from these

observations that: (i) The $D_{14}D_{20}$ combination band is inherently bright; and (ii) there is no evidence that it interacts significantly with the $D_{30}$ vibration (under $C_{2v}$ symmetry, where their symmetry is the same).

### *4.* $D_{11}$ and $D_{29}$

We also note that the intensity of the equivalent of the $D_{11}$ band relative to the origin band is very variable in the REMPI spectra across different substituted benzenes. For example, in the case of fluorobenzene it is exceptionally weak,[59,63] and it appears to be more intense in chlorobenzene[60] than in bromobenzene;[61] also, as Figure 2 shows, the $D_{11}$ band is relatively more intense in the case of *p*DFB than for *p*FT. Further, there appear to be similar variations in the relative intensities of the HT-allowed $D_{29}$ band, although in the specific comparison between *p*DFB and *p*FT the overlapping bands in the latter mean that we are unsure of how much band intensity is due to $29_0^1$ and how much is due to $14_0^2$. As mentioned above, and discussed by Blease et al.,[49] some indication of FC activity can be ascertained by comparing the same electronic transition recorded using one- and two-photon excitation REMPI spectroscopy. Intensities that remain relatively unaltered may be deemed to be representative of FC activity, while those that change dramatically are indicative of HT-activity[49] (to which we note that some consideration may also need to be given to enhancements at the one-photon virtual level in the two-photon spectrum). For *p*-xylene[49] and in phenylsilane,[50] we note that significant differences in intensities are seen between the one- and two-photon REMPI spectra, involving the expected $b_2$ symmetry vibrations, but also the $a_1$ symmetry ones. We take this as evidence that the $A_1$ and $B_2$ components of the

equivalent of the $\tilde{C}\ ^1E_{1u}$ state of benzene in substituted benzenes each affect observed intensities in the $S_1 \leftarrow S_0$ transition, and in particular that $a_1$ symmetry vibrations have both FC and HT intensity contributions. (This may explain why it has always been difficult to simulate intensities of the $S_1 \leftarrow S_0$ transition in substituted benzenes, since HT coupling is almost always omitted: not only are all of the $b_2$ symmetry levels absent, but also the intensities of the $a_1$ vibrations can be incorrect, depending on how much of their intensity comes from a HT contribution.)

**VII. CONCLUSIONS**

In this paper we have investigated in detail the ZEKE spectra recorded *via* a large number of $S_1$ torsion, vibtor and vibrational levels of *p*FT, accessed via transitions with wavenumbers in the range 0–570 $cm^{-1}$. (A summary of bands observed in the various ZEKE spectra is provided as Supplementary Material.)[64] As a result of this, we have able to confirm the presence of torsion-vibrational coupling in the $S_1$ state and that a number of the observed transitions in the REMPI spectrum arise from vibtor levels; as a consequence, we also expect such interactions in the cation. A complete treatment of the torsion-vibrational coupling is presented in an accompanying paper,[39] which also includes results from the accompanying 2D-LIF study.[38] What is clear from the results here is that the vibration-torsional coupling is pervasive and involves different vibrations, with the symmetry of the vibration dictating which *m* levels can interact. Further, subsequent interactions between the vibtor levels and vibrational states can lead to eigenstates that are admixtures of these, and hence provide generalized routes for energy flow between torsional and vibrational motions and hence, as discussed by (amongst others) Parmenter et al.[1,23,24,25,31,35], Reid and Davies[28] and Gascooke et al.,[14] accelerated IVR in methyl-group-containing molecules. We also deduce that the

vibration-torsional coupling is subtly different for each of the vibrational levels (fundamentals, combinations and overtones), as expected. We also note that when comparing molecules, particularly those that have different symmetries, the form of the vibrations may change significantly. As well as changing the wavenumber and the symmetry (where a lowering would result in further potential for interactions), this can significantly change the form of the vibrations, and hence the couplings between them: we highlight that the form of some of the stretch vibrations of *p*DFB ($D_{2h}$) evolve into localized vibrational modes in the *para*-disubstituted species,[40] for example.

As a part of the present study, we have investigated the pair of features at ~ 405 $cm^{-1}$ and have shown that there is the possibility of a weak Fermi resonance between the $D_{11}$ and $2D_{14}$ levels, and that there is likely an interaction between the $2D_{14}$ and $D_{14}$ $m$ = 6(-) levels, although again this appears to be weak. (Each of these conclusions implicitly assumes there is no other photophysical depletion mechanism occurring on the ns timescale of our experiments.)

Additionally, we have concluded that for *p*FT and, we have hypothesised, also for all substituted benzenes, Herzberg-Teller intensity stealing occurs not only for the commonly-discussed $b_2$ symmetry vibrations, but also for $a_1$ vibrations. Such considerations explain the very different activity observed for various vibrations in the $S_1 \leftarrow S_0$ spectra, but particularly the $D_{29}$ and $D_{11}$ vibrations. In passing, we note that in phenylsilane[50] the totally-symmetric ($a_1$) vibration labelled as $\nu_1$ in that work is very intense in the one-colour spectrum, but almost completely vanishes in the two-colour spectrum; hence exhibiting very similar behaviour to the non-totally-symmetric ($b_2$) $D_{29}$ (labelled $\nu_{6b}$ therein) vibration. From this general behaviour we have gained insight into the activity of the $m$ = 3(+) and $m$ = 3(-) torsional levels.

We conclude that the $m$ = 3(+) level is active in the $S_1 \leftarrow S_0$ transition from a breakdown of the Born-Oppenheimer approximation in the $S_1$ state, in agreement with the established explanation; however, we suggest that this mechanism also occurs in the $D_0^+$ state, and that this leads to activity in the $m$ = 3(-) torsion when ionizing via the origin of the $S_1$ state. However, for some molecules, it is clear that the $m$ = 3(+) level is clearly seen, but we have noted that for phenylsilane[50,57] the $D_{29}$ vibration is also unexpectedly active alongside the $m$ = 3(+). This observation, together with the more general comments on HT coupling, lead us to suggest that for some molecules, the splitting between the two lowest energy cation electronic states, which are both derived from the same degenerate state of benzene, is driving the activity in these $b_2$ ($a_1''$) modes/torsions. We believe this is the case for both phenylsilane[57] and for 2,6-dFT;[62] additionally, if a $m$ = 3(+) transition has reasonable intensity, then rotation-torsional coupling can lead to some intensity being transferred to the $m$ = 3(-) level, enhancing its intensity.

Finally, we note that there are some remarkable coincidences in transition wavenumber for this molecule, which have made the interpretation interesting to unravel. This is often compounded by the similarity in wavenumber and thus similarity of the eigenstates in the $S_1$ state and in the cation, making disentangling the coupling between torsions and vibtors from the ZEKE spectra problematic. Fortunately, with the combined results of quantum chemical calculations, the ZEKE activity in the present work, and the 2D-LIF activity in the forthcoming paper[38] the assignments are secure in almost all cases. One region where there is some uncertainty is the "ripples" leading up to the two main ~405 $cm^{-1}$ features, where contributions from cold *p*FT bands, hot *p*FT bands as well as the two complexes, *p*FT-Ar and *p*FT-$Ar_2$, complicate the definitive assignments of some of those features; but sound

conclusions have been reached. In future work, we hope to gain further insight into these by the recording of ZEKE spectra for the complexes via different intermediate intermolecular vibrational levels.

**Supplementary Material**

See supplementary material for a summary of the wavenumbers and assignments of the ZEKE bands seen when exciting through various $S_1$ intermediate states.

**Acknowledgements**

We are grateful to the EPSRC for funding (grant EP/L021366/1). The EPSRC and the University of Nottingham are thanked for studentships to W.D.T. and L.W. We are grateful to the NSCCS for the provision of computer time under the auspices of the EPSRC, and to the High Performance Computer resource at the University of Nottingham. The work in the present paper has greatly benefitted from discussions with Warren Lawrance and Jason Gascooke (Adelaide); we also gratefully acknowledge conversations with Katharine Reid (Nottingham) and Julia Davies (Imperial College/Nottingham).

**Table I**: Vibrational labelling schemes together with calculated and experimental values for the vibrational wavenumbers of *p*FT in the $S_1$ and $D_0^+$ states (both staggered conformation – see text).

| $D_i$ [a] | Wilson/Varsányi [b] | Mixed (Bz) [c] | Mulliken (Methyl-$C_{2v}$) [d] | Mulliken ($D_{2h}$) [e] | $S_1$ | | $D_0^+$ | |
|---|---|---|---|---|---|---|---|---|
| | | | | | Calc [f] | Expt [g] | Calc [h] | Expt [g] |
| | | | ***a*$_1$** | | | | | |
| $D_1$ | 2 | **2**,7a | 1 | 1($a_g$) | 3130 | | 3116 | |
| $D_2$ | 20*a* | **13**,20a | 2 | 10($b_{1u}$) | 3105 | | 3101 | |
| $D_3$ | 8*a* | **9a** | 4 | 2($a_g$) | 1528 | | 1628 | 1631 |
| $D_4$ | 19*a* | **18a**,(20a) | 5 | 11($b_{1u}$) | 1432 | | 1454 | |
| $D_5$ | 7*a* | 1,7a,(2,6a) | 7 | 3($a_g$) | 1213 | 1230 | 1311 | 1332 |
| $D_6$ | 13 | 12,19a,20a,(13 18a) | 8 | 12($b_{1u}$) | 1185 | 1194 | 1211 | 1230 |
| $D_7$ | 9*a* | **8a** | 9 | 4($a_g$) | 1120 | | 1158 | 1170 |
| $D_8$ | 18*a* | **19a**,12 | 10 | 13($b_{1u}$) | 954 | [i] | 969 | [i] |
| $D_9$ | 1 | **1**,6a,(7a,2) | 11 | 5($a_g$) | 805 | 803 | 811 | 834 |
| $D_{10}$ | 12 | 20a,12,(19a,13) | 12 | 14($b_{1u}$) | 700 | [i] | 710 | [i] |
| $D_{11}$ | 6a | **6a**,7a,(2,1) | 13 | 6($a_g$) | 410 | 408 | 437 | 440 |
| | | | ***a*$_2$** | | | | | |
| $D_{12}$ | 17*a* | **17a** | 14 | 7($a_u$) | 588 | | 987 | |
| $D_{13}$ | 10*a* | **10a** | 15 | 9($b_{1g}$) | 484 | | 770 | |
| $D_{14}$ | 16*a* | **16a** | 16 | 8($a_u$) | 172 | 199 | 356 | 350 |
| | | | ***b*$_1$** | | | | | |
| $D_{15}$ | 5 | **5**,10b | 20 | 15($b_{2g}$) | 706 | | 998 | |
| $D_{16}$ | 17*b* | **17b**,11,(16b) | 21 | 28($b_{3u}$) | 651 | | 832 | |
| $D_{17}$ | 4 | **4**,(10b) | 22 | 16($b_{2g}$) | 538 | | 671 | |
| $D_{18}$ | 16*b* | **16b**,11,(17b) | 23 | 29($b_{3u}$) | 468 | 435 | 488 | |
| $D_{19}$ | 10*b* | **10b**,(4,5) | 24 | 17($b_{2g}$) | 243 | 242[j,k] | 266 | 271[j] |
| $D_{20}$ | 11 | 16b,17b,11 | 25 | 30($b_{3u}$) | 110 | 110[j,k] | 109 | 111[j] |
| | | | ***b*$_2$** | | | | | |
| $D_{21}$ | 7*b* | **20b** | 26 | 18($b_{2u}$) | 3126 | | 3115 | |
| $D_{22}$ | 20*b* | **7b** | 27 | 23($b_{3g}$) | 3100 | | 3101 | |
| $D_{23}$ | 8*b* | **9b** | 29 | 24($b_{3g}$) | 1427 | | 1383 | |
| $D_{24}$ | 19*b* | **18b**,(19b,14,15) | 31 | 19($b_{2u}$) | 1315 | | 1470 | |
| $D_{25}$ | 14 | **15**,(14) | 32 | 20($b_{2u}$) | 935 | | 1301 | |
| $D_{26}$ | 3 | **3**,8b | 33 | 25($b_{3g}$) | 1255 | | 1250 | |
| $D_{27}$ | 18*b* | **14**,19b | 34 | 21($b_{2u}$) | 1053 | | 1115 | |
| $D_{28}$ | 6*b* | **6b**,(8b) | 36 | 26($b_{3g}$) | 546 | 549 | 564 | 570 |
| $D_{29}$ | 9*b* | 8b,6b,(3) | 37 | 27($b_{3g}$) | 395 | 399 | 412 | 416 |
| $D_{30}$ | 15 | 19b,14,(18b) | 38 | 22($b_{2u}$) | 307 | 311[j] | 313 | 320[j] |

[a] Labelling scheme from ref. 40

[b] These labels are those used in ref. 37, but similar labels have been used in other work, they derive from the work of Varsányi,[41] who used Wilson-type labels. As may be seen by comparing to the mixed labels in the subsequent column, Wilson labels are far from satisfactory. (See ref. 40 for further discussion.)

[c] Normal modes of *p*FT ($D_i$ modes) expressed in terms of those of benzene (Wilson modes) using a generalized Duschinsky approach applied to *p*DFB for which one F atom has been artificially changed to mass 15 amu – see ref. 40. Values outside parentheses have mixing coefficients > 0.2 and are termed major contributions, with bolded values being dominant contributions (mixing coefficients > 0.5). Those inside parentheses are minor contributions, and have values between 0.05 and 0.2. If there is more than one contribution of each type, these are given in numerical order. Vibrations with a mixing coefficient < 0.05 are ignored.

[d] These are Mulliken labels assuming that the molecule can be considered as having $C_{2v}$ symmetry and appear to have been used first in ref. 6; however, methyl-localized vibrations were included in that list, which cannot be given $C_{2v}$ symmetry labels. (Additionally, the point group symmetry will depend on the orientation of the methyl group, further complicating matters.) These labels were also used in ref. 37 and other work on *p*FT; this use should be dropped.

[e] Mulliken labels that apply to a $D_{2h}$ molecule, such as *p*DFB, using the standard ordering (see ref. 40 for a discussion of these and their relation to the other labels).

[f] Calculated using TDDFT: B3LYP/aug-cc-pVTZ, and values scaled by 0.97.

[g] Values taken from ref. 37 and/or discussed in the text.

[h] Calculated using B3LYP/aug-cc-pVTZ, and values scaled by 0.97.

[i] A value was assigned to this vibration in ref. 37, but this assignment is now thought to be questionable and will be discussed in a forthcoming paper.[55]

[j] This value is a reassignment in the present work of a value in ref. 37 – see text.

[k] This value is half of the overtone value; however, the value of the fundamental will need to be extracted from band positions that are affected by vibration-torsion interactions.

**Table II:** Allowed combinations of vibration and torsion to give vibtor levels of the correct symmetry to be either Franck-Condon or Herzberg-Teller allowed in the $S_1$ state – see also Table 1.

| Vibrational Symmetry ($C_{2v}$) | Torsional level | Torsional symmetry ($G_{12}$) |
|---|---|---|
| $a_1'$ overall vibtor symmetry – Franck-Condon allowed | | |
| $a_1$ | 0, 6(+) | $a_1'$ |
| $b_2$ | 3(+) | $a_1''$ |
| $a_2$ | 6(-) | $a_2'$ |
| $b_1$ | 3(-) | $a_2''$ |
| $a_1''$ overall vibtor symmetry – Herzberg-Teller allowed | | |
| $a_1$ | 3(+) | $a_1''$ |
| $b_2$ | 0, 6(+) | $a_1'$ |
| $a_2$ | 3(-) | $a_2''$ |
| $b_1$ | 6(-) | $a_2'$ |

**Table III:** Combined symmetries of vibtor levels arising from selected vibrations

| *m* | Pure Torsion | $D_{20}$ ($A_2''$) vibtor | $D_{14}$ ($A_2'$) vibtor | $D_{19}$ ($A_2''$) vibtor | $2D_{20}$ ($A_1'$) vibtor | $D_{30}$ ($A_1''$) vibtor |
|---|---|---|---|---|---|---|
| 0 | $a_1'$ | $a_2''$ | $a_2'$ | $a_2''$ | $a_1'$ | $a_1''$ |
| 1 | $e''$ | $e'$ | $e''$ | $e'$ | $e''$ | $e'$ |
| 2 | $e'$ | $e''$ | $e'$ | $e''$ | $e'$ | $e''$ |
| 3(+) | $a_1''$ | $a_2'$ | $a_2''$ | $a_2'$ | $a_1''$ | $a_1'$ |
| 3(-) | $a_2''$ | $a_1'$ | $a_1''$ | $a_1'$ | $a_2''$ | $a_2'$ |
| 4 | $e'$ | $e''$ | $e'$ | $e''$ | $e'$ | $e''$ |
| 5 | $e''$ | $e'$ | $e''$ | $e'$ | $e''$ | $e'$ |
| 6(+) | $a_1'$ | $a_2''$ | $a_2'$ | $a_2''$ | $a_1'$ | $a_1''$ |
| 6(-) | $a_2'$ | $a_1''$ | $a_1'$ | $a_1''$ | $a_2'$ | $a_2''$ |
| 7 | $e''$ | $e'$ | $e''$ | $e'$ | $e''$ | $e'$ |

**Figure Captions**

Figure 1: Correlation of the $D_{6h}$ point group symmetry classes to those of the $C_{2v}$ point group, with the indicated axis systems. In addition, the molecular symmetry group classes are given for the $G_{12}$ group and, where they exist, the equivalences are given to the $C_{2v}$ ones. Note that the (*x, y, z*) axis system is not uniquely defined in general for the $C_{2v}$ point group. The *a, b, c* axis system for the $G_{12}$ molecular symmetry group is the principal axis system. Note that there are no equivalences of the *e*′ and *e*″ molecular symmetry labels in the $C_{2v}$ point group.

Figure 2: Low-wavenumber region of the REMPI spectra of: (a) *p*FT (upright); and (b) *p*DFB (inverted). Assignments given are discussed in the text. In these spectra we have given the $S_0$ (lower) and $S_1$ (upper) quantum levels for each vibration and torsion. The wavenumber scale is relative to the origin of the $S_1 \leftarrow S_0$ transition at 36859.9 $cm^{-1}$. The label with a bar over it refers to the *p*FT-Ar complex.

Figure 3: ZEKE spectrum recorded via the $S_1$ $m$ = 0 and $S_1$ $m$ = 1 levels. Both $m$ levels are accessed as the two transition wavenumbers are within our laser resolution; further, the two lowest $m$ levels have different nuclear spin states and so both remain populated in the jet expansion. Assignments are discussed in the text. In this spectrum we have given the $S_1$ (lower) and $D_0^+$ (upper) quantum levels for each vibration and torsion. For REMPI spectra the wavenumber scale is relative to the origin of the $S_1 \leftarrow S_0$ transition at 36859.9 $cm^{-1}$, while for the ZEKE spectra the wavenumber scales are relative to the adiabatic ionization of *p*FT at 70946 $cm^{-1}$.

Figure 4: Trace (a) shows a portion of the REMPI spectrum, showing the relevant transitions employed to access these levels. Other traces show ZEKE spectra recorded via the (b) $S_1$ 0 $m$ = 0 and 1; (c) $S_1$ 0 $m$ = 2; (d) $S_1$ 0 $m$ = 3(+); and (e) $S_1$ 0 $m$ = 4 levels. Assignments are discussed in the text. For the REMPI spectrum the wavenumber scale is relative to the origin of the $S_1 \leftarrow S_0$ transition at 36859.9 $cm^{-1}$, while for the ZEKE spectra the wavenumber scales are relative to the adiabatic ionization of *p*FT at 70946 $cm^{-1}$.

Figure 5: ZEKE spectra in the region of the $m$ = 3(+) and 3(-) levels recorded at slightly difference excitation wavenumbers (indicated in the REMPI spectrum on the right-hand side of the figure and using colour coding) and hence exciting different portions of the rotational envelope of the underlying transitions. Upper (upright) trace: via the $S_1$ $m$ = 0 level. Lower (inverted) trace via the $S_1$ $m$ = 3(+) level. For the REMPI spectra the wavenumber scale is relative to the origin of the $S_1 \leftarrow S_0$ transition at 36859.9 $cm^{-1}$, while for the ZEKE spectra the wavenumber scales are relative to the adiabatic ionization of *p*FT at 70946 $cm^{-1}$.

Figure 6: Trace (a) shows a portion of the REMPI spectrum, showing the relevant transitions/ excitation positions employed to access these levels. Other traces show ZEKE spectra recorded via: (b-d) three different excitation positions of the transition to the $D_{20}$ $m$ = 2…$m$ = 5 level; and (e) the $m$ = 5…$D_{20}$ $m$ = 2 level. The ZEKE spectrum in trace (c) also shows evidence of $D_{20}$ $m$ = 1. Assignments are discussed in the text. For the REMPI spectrum the wavenumber scale is relative to the origin of the $S_1 \leftarrow S_0$ transition at 36859.9 $cm^{-1}$, while for

the ZEKE spectra the wavenumber scales are relative to the adiabatic ionization of *p*FT at 70946 $cm^{-1}$. The band whose assignment is in square brackets does not originate from the given intermediate, but from an overlap with another feature at this wavenumber (see text). The colour in this figure is used just for clarity.

Figure 7: Trace (a) shows a portion of the REMPI spectrum, showing the relevant transitions employed to access these levels. Other traces show ZEKE spectra recorded via each of the levels: (b) $D_{20}$ $m$ = 3(-); (c) $D_{20}$ $m$ = 4; and (d) $2D_{20}$. Assignments are discussed in the text. For the REMPI spectrum the wavenumber scale is relative to the origin of the $S_1 \leftarrow S_0$ transition at 36859.9 $cm^{-1}$, while for the ZEKE spectra the wavenumber scales are relative to the adiabatic ionization of *p*FT at 70946 $cm^{-1}$.

Figure 8: Trace (a) shows a portion of the REMPI spectrum, showing the relevant transitions employed to access these levels. Trace (b) shows a ZEKE spectrum recorded via the feature at 196 $cm^{-1}$ assigned as being overlapped bands associated with $S_1$ $m$ = 6(+) and $D_{14}$; other results suggest that the latter state likely has a small contribution from $m$ = 6(-). See text for further discussion. For the REMPI spectrum the wavenumber scale is relative to the origin of the $S_1 \leftarrow S_0$ transition at 36859.9 $cm^{-1}$, while for the ZEKE spectrum the wavenumber scales are relative to the adiabatic ionization of *p*FT at 70946 $cm^{-1}$.

Figure 9: Trace (a) shows a portion of the REMPI spectrum, showing the relevant transitions employed to access these levels. Other traces show ZEKE spectra recorded via each of the

levels: (b) $D_{19}$ $m$ = 2 and $m$ =7 (via overlapping region); (c) $D_{19}$ $m$ = 2; (d) $D_{19}$ $m$ = 3(-); and (e) $D_{19}$ $m$ = 4. Assignments are discussed in the text. For the REMPI spectrum the wavenumber scale is relative to the origin of the $S_1 \leftarrow S_0$ transition at 36859.9 $cm^{-1}$, while for the ZEKE spectra the wavenumber scales are relative to the adiabatic ionization of *p*FT at 70946 $cm^{-1}$.

Figure 10: Trace (a) shows a portion of the REMPI spectrum, showing the relevant excitation positions employed to access these levels, the bands marked with asterisks are due to fragmentation of the pFT-Ar complex; two-colour, mass-resolved spectra of these are given in Figure 11. Other traces show ZEKE spectra recorded via: (b-d) three excitation wavelengths corresponding to the overlapped $D_{30}/D_{14}D_{20}/D_{20}m$ = 6(-) levels; and (e) the $D_{14}$ $m$ = 6(-) level. Other results suggest that the latter state likely has a small contribution from the $D_{14}$ overtone. See text for further discussion. For the REMPI spectrum the wavenumber scale is relative to the origin of the $S_1 \leftarrow S_0$ transition at 36859.9 $cm^{-1}$, while for the ZEKE spectra the wavenumber scales are relative to the adiabatic ionization of *p*FT at 70946 $cm^{-1}$.

Figure 11: Two-colour REMPI spectra recorded when gating the mass channels corresponding to: (a) *p*FT; (b) *p*FT-Ar; and (c) *p*FT-$Ar_2$. The wavenumber scale is relative to the origin of the $S_1 \leftarrow S_0$ transition at 36859.9 $cm^{-1}$. The region marked by an asterisk in the *p*FT-$Ar_2$ spectrum is omitted owing to severe interference from uncomplexed *p*FT at this wavenumber, which could not be successfully subtracted.

Figure 12: ZEKE spectra recorded at different excitation wavenumbers across the 395–415 $cm^{-1}$ region. Assignments are discussed in the text. The vertical trace on the right-hand side shows the REMPI spectrum over this range, with the dashed lines linking the excitation position to the relevant ZEKE spectrum. See also Figure 13. For the REMPI spectrum the wavenumber scale is relative to the origin of the $S_1 \leftarrow S_0$ transition at 36859.9 $cm^{-1}$, while for the ZEKE spectra the wavenumber scales are relative to the adiabatic ionization of *p*FT at 70946 $cm^{-1}$.

Figure 13: Trace (a) shows a portion of the REMPI spectrum, showing the relevant transitions employed to access these levels. Other traces show ZEKE spectra recorded via the following levels: (b) $D_{14}$ $m$ = 6(+); (c) predominantly the $D_{14}$ overtone; and (d) the $D_{19}$ overtone. Assignments are discussed in the text. The bands marked with asterisks are due to fragmentation of pFT/Ar complexes; two-colour, mass-resolved spectra of these are given in Figure 11. The insert shows an overlay of a narrow region the three spectra to emphasise that indeed there are two distinct bands here. For the REMPI spectrum the wavenumber scale is relative to the origin of the $S_1 \leftarrow S_0$ transition at 36859.9 $cm^{-1}$, while for the ZEKE spectra the wavenumber scales are relative to the adiabatic ionization of *p*FT at 70946 $cm^{-1}$.

**Figure 1:**

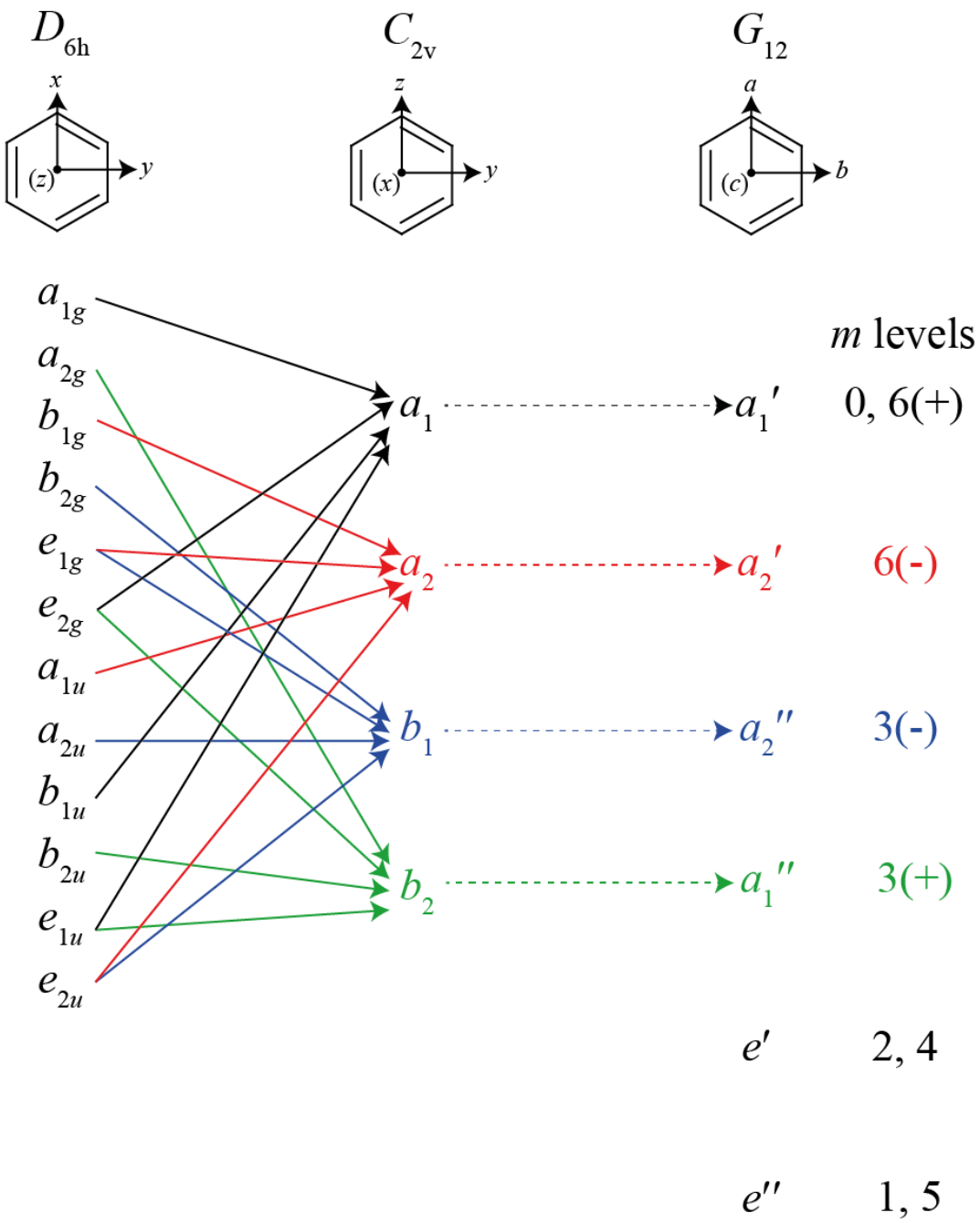
D6h
C2v
G12
x
y
(z)
z
y
(x)
a
b
(c)
a1g
a2g
b1g
b2g
e1g
e2g
a1u
a2u
b1u
b2u
e1u
e2u
a1
a2
b1
b2
m levels
a1′ 0, 6(+)
a2′ 6(-)
a2″ 3(-)
a1″ 3(+)
e′ 2, 4
e″ 1, 5

**Figure 2**

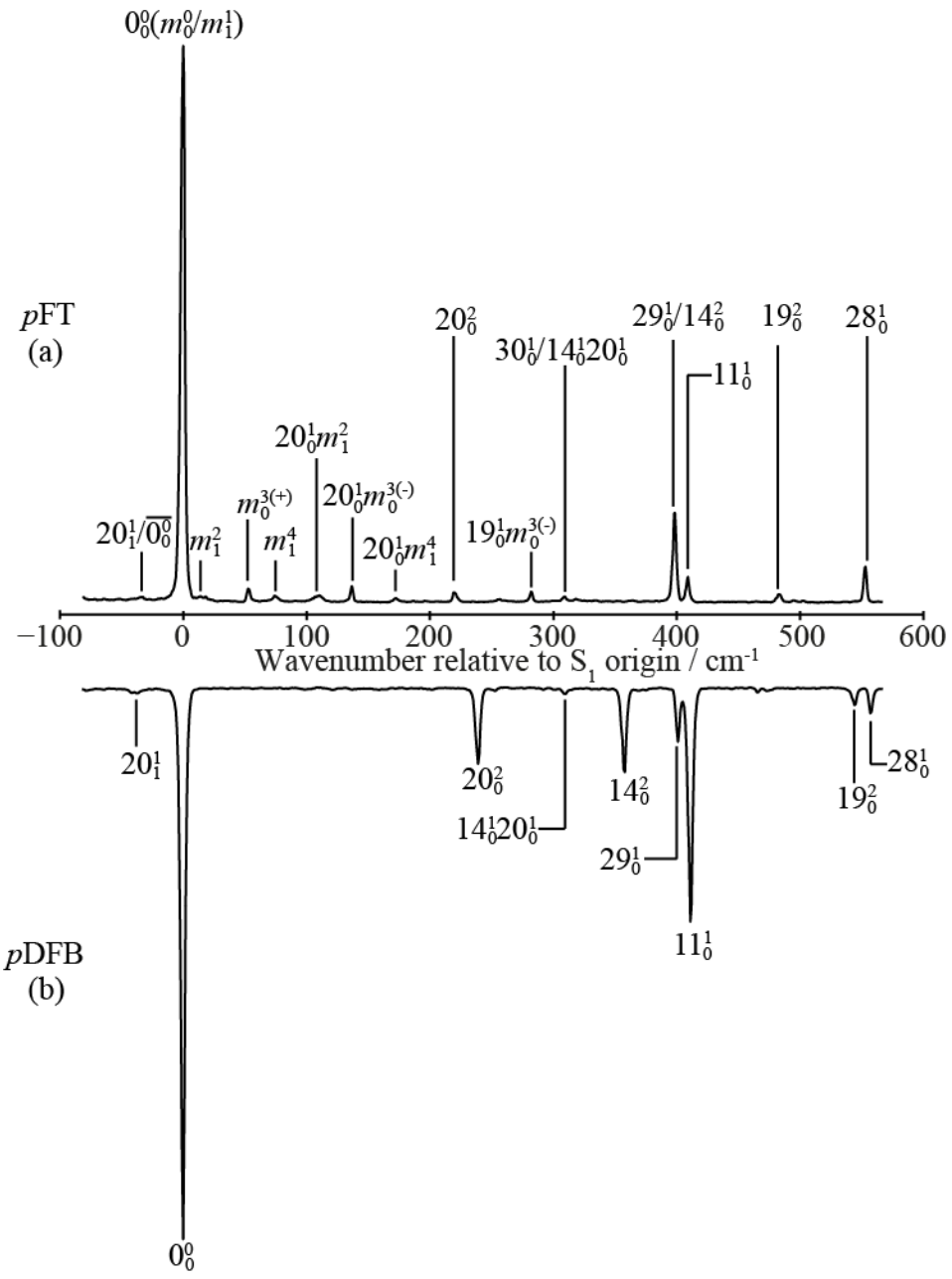
$0_0^0(m_0^0/m_1^1)$
pFT
(a)
$20_0^2$
$30_0^1/14_0^120_0^1$
$29_0^1/14_0^2$
$19_0^2$
$28_0^1$
$11_0^1$
$20_0^1m_1^2$
$20_0^1m_0^{3(-)}$
$m_0^{3(+)}$
$20_1^1/\overline{0_0^0}$
$m_1^2$
$m_1^4$
$20_0^1m_1^4$
$19_0^1m_0^{3(-)}$
−100
0
100
200
300
400
500
600
Wavenumber relative to $S_1$ origin / $cm^{-1}$
$20_1^1$
$20_0^2$
$14_0^120_0^1$
$14_0^2$
$29_0^1$
$11_0^1$
$19_0^2$
$28_0^1$
pDFB
(b)
$0_0^0$

**Figure 3**

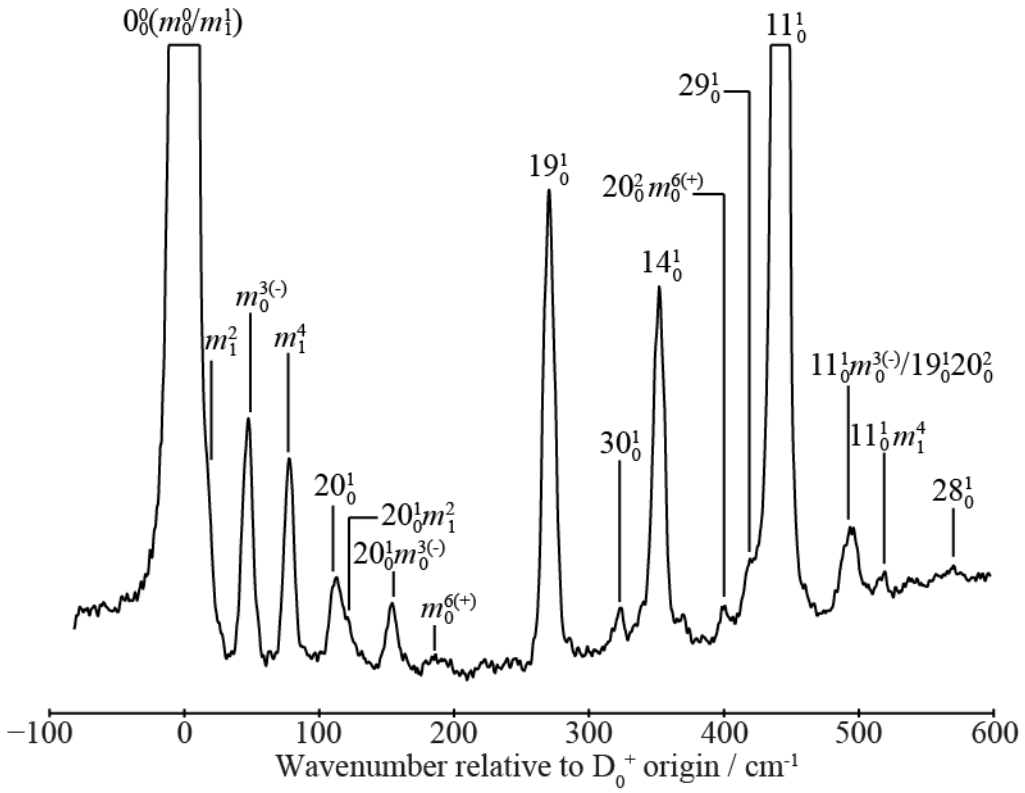
$0_0^0(m_0^0/m_1^1)$
$m_1^2$
$m_0^{3(-)}$
$m_1^4$
$20_0^1$
$20_0^1m_1^2$
$20_0^1m_0^{3(-)}$
$m_0^{6(+)}$
$19_0^1$
$20_0^2m_0^{6(+)}$
$14_0^1$
$30_0^1$
$29_0^1$
$11_0^1$
$11_0^1m_0^{3(-)}/19_0^120_0^2$
$11_0^1m_1^4$
$28_0^1$
−100
0
100
200
300
400
500
600
Wavenumber relative to $D_0^+$ origin / $cm^{-1}$

**Figure 4**

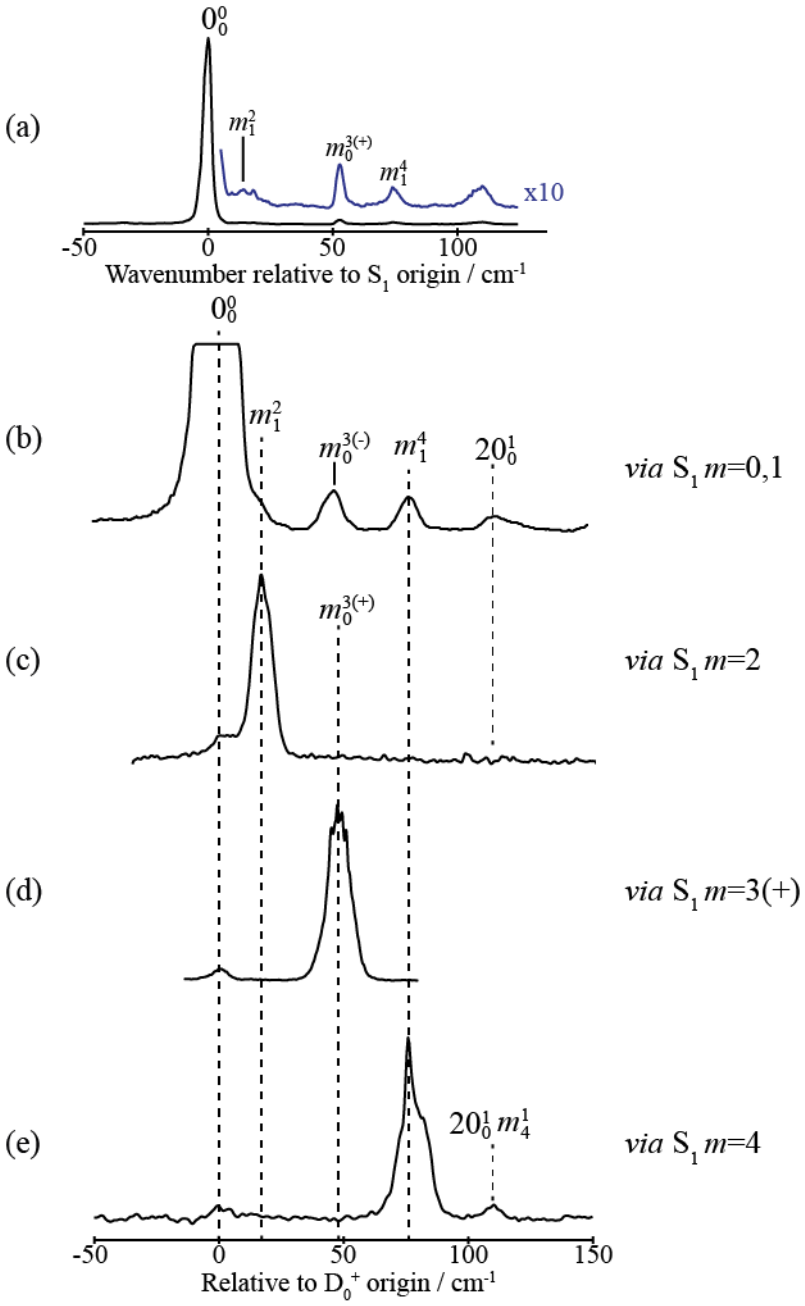
(a)
$0_0^0$
$m_1^2$
$m_0^{3(+)}$
$m_1^4$
x10
-50
0
50
100
Wavenumber relative to $S_1$ origin / $cm^{-1}$
(b)
$0_0^0$
$m_1^2$
$m_0^{3(-)}$
$m_1^4$
$20_0^1$
*via* $S_1$ *m*=0,1
(c)
$m_0^{3(+)}$
*via* $S_1$ *m*=2
(d)
*via* $S_1$ *m*=3(+)
(e)
$20_0^1 m_4^1$
*via* $S_1$ *m*=4
-50
0
50
100
150
Relative to $D_0^+$ origin / $cm^{-1}$

**Figure 5**

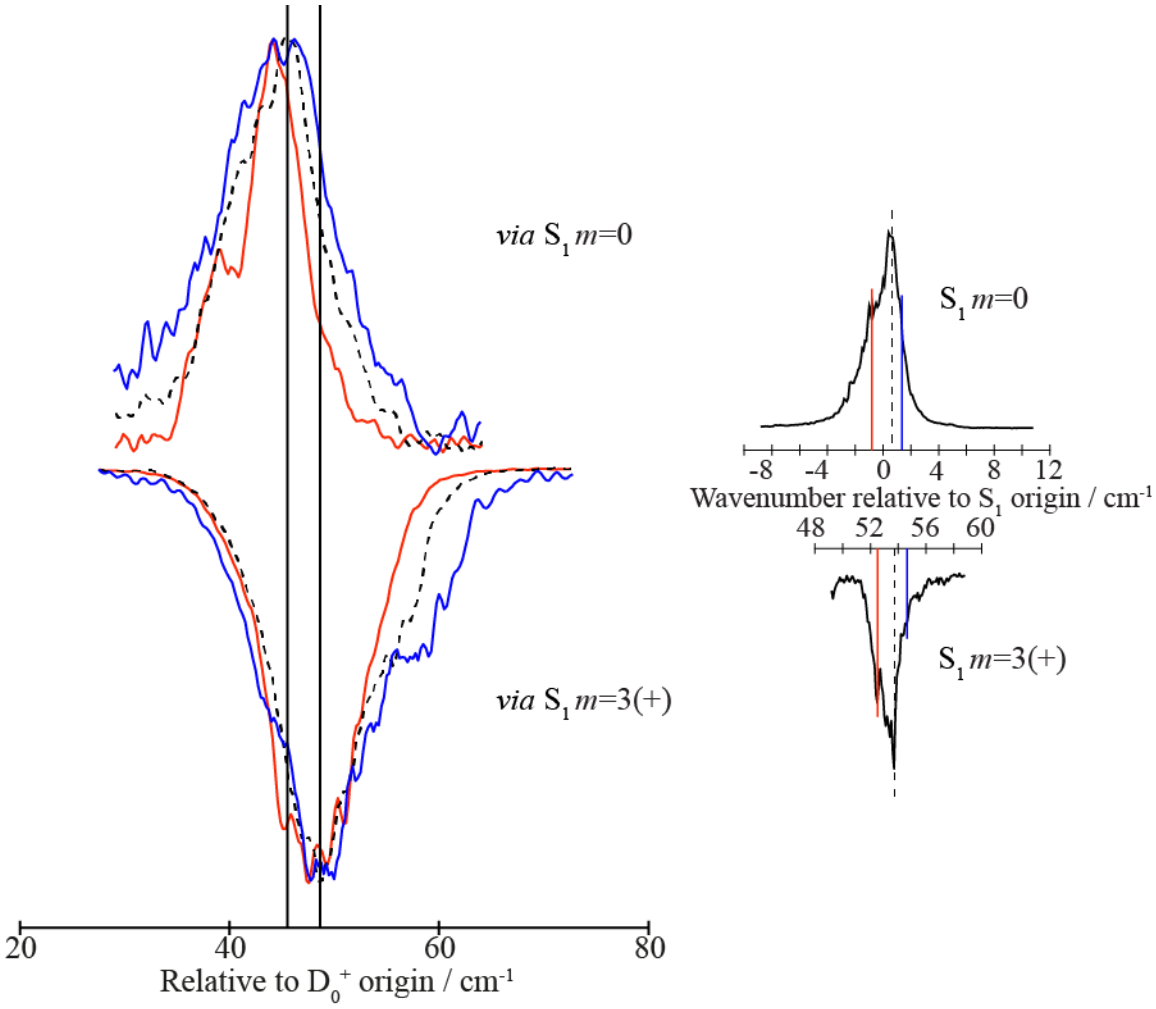
via S1 m=0
via S1 m=3(+)
20
40
60
80
Relative to D0+ origin / cm-1
S1 m=0
-8
-4
0
4
8
12
Wavenumber relative to S1 origin / cm-1
48
52
56
60
S1 m=3(+)

**Figure 6**

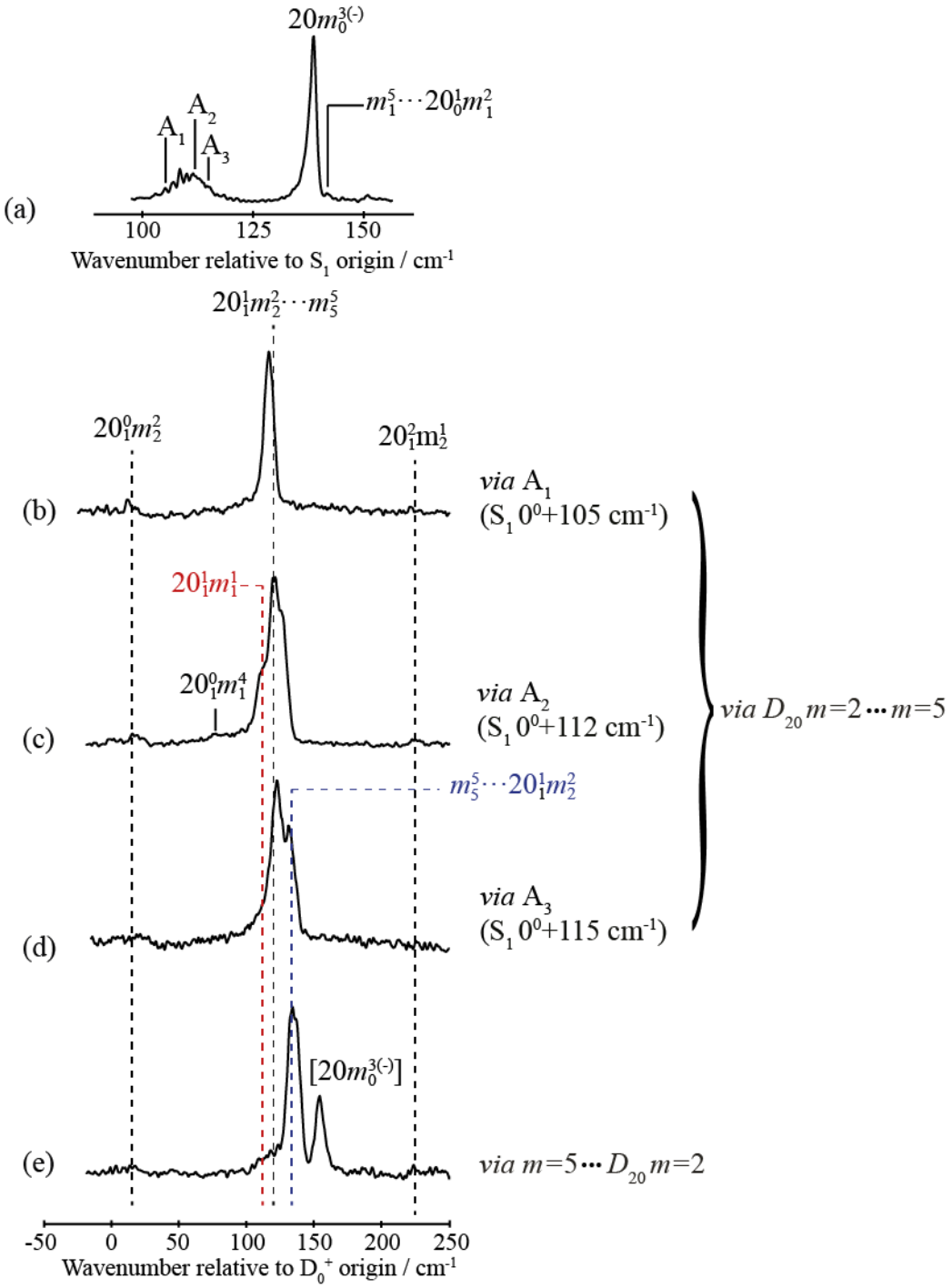
$20m_0^{3(-)}$
$m_1^5\cdots 20_0^1m_1^2$
A1
A2
A3
(a)
100
125
150
Wavenumber relative to S1 origin / cm-1
$20_1^1m_2^2\cdots m_5^5$
$20_1^0m_2^2$
$20_1^2m_2^1$
(b)
via A1
(S1 00+105 cm-1)
$20_1^1m_1^1$
$20_1^0m_1^4$
(c)
via A2
(S1 00+112 cm-1)
via D20 m=2⋯m=5
$m_5^5\cdots 20_1^1m_2^2$
(d)
via A3
(S1 00+115 cm-1)
$[20m_0^{3(-)}]$
(e)
via m=5⋯D20 m=2
-50
0
50
100
150
200
250
Wavenumber relative to D0+ origin / cm-1

**Figure 7**

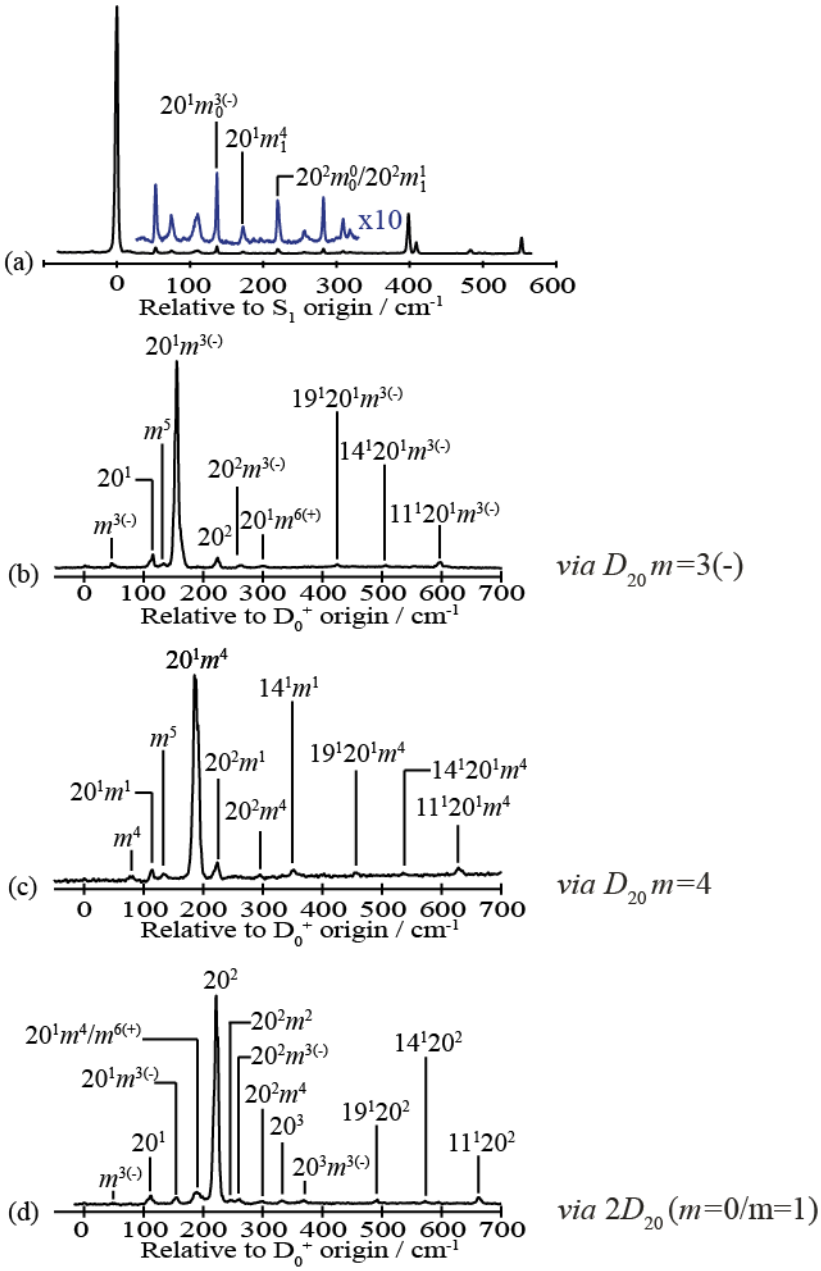


*via* $D_{20}$ $m$=3(-)

*via* $D_{20}$ $m$=4

*via* $2D_{20}$ ($m$=0/m=1)

**Figure 8**

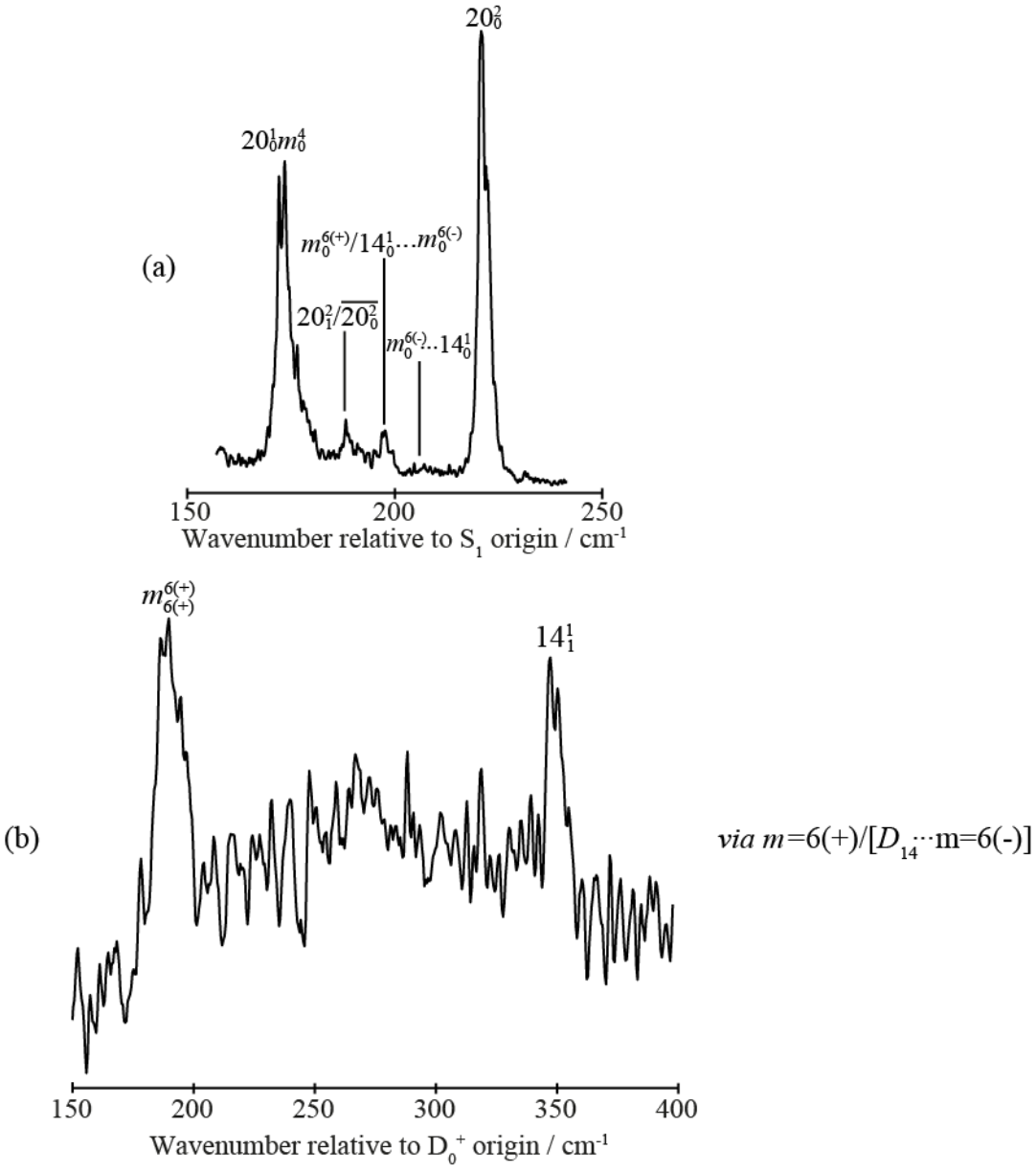


*via* $m$=6(+)/[$D_{14}$···m=6(-)]

**Figure 9**

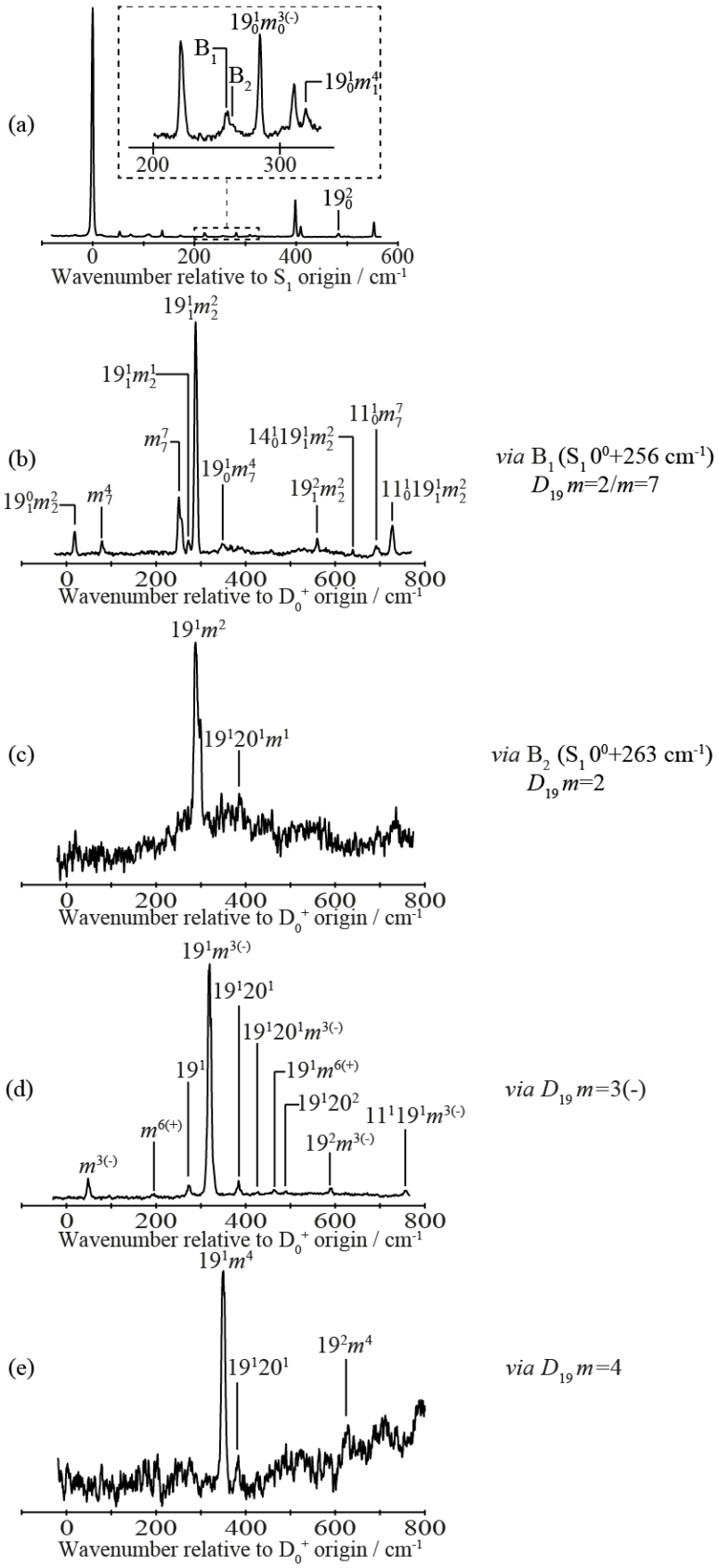
(a)
$19_0^1m_0^{3(-)}$
$B_1$
$B_2$
$19_0^1m_1^4$
200
300
$19_0^2$
0
200
400
600
Wavenumber relative to $S_1$ origin / cm$^{-1}$
(b)
$19_1^1m_2^2$
$19_1^1m_2^1$
$m_7^7$
$14_0^119_1^1m_2^2$
$11_0^1m_7^7$
$19_0^1m_7^4$
$19_1^0m_2^2$
$m_7^4$
$19_1^2m_2^2$
$11_0^119_1^1m_2^2$
0
200
400
600
800
Wavenumber relative to $D_0^+$ origin / cm$^{-1}$
*via* $B_1$ ($S_1$ $0^0$+256 cm$^{-1}$)
$D_{19}$ $m$=2/$m$=7
(c)
$19^1m^2$
$19^120^1m^1$
0
200
400
600
800
Wavenumber relative to $D_0^+$ origin / cm$^{-1}$
*via* $B_2$ ($S_1$ $0^0$+263 cm$^{-1}$)
$D_{19}$ $m$=2
(d)
$19^1m^{3(-)}$
$19^120^1$
$19^120^1m^{3(-)}$
$19^1$
$19^1m^{6(+)}$
$19^120^2$
$11^119^1m^{3(-)}$
$m^{6(+)}$
$19^2m^{3(-)}$
$m^{3(-)}$
0
200
400
600
800
Wavenumber relative to $D_0^+$ origin / cm$^{-1}$
*via* $D_{19}$ $m$=3(-)
(e)
$19^1m^4$
$19^2m^4$
$19^120^1$
0
200
400
600
800
Wavenumber relative to $D_0^+$ origin / cm$^{-1}$
*via* $D_{19}$ $m$=4

**Figure 10**

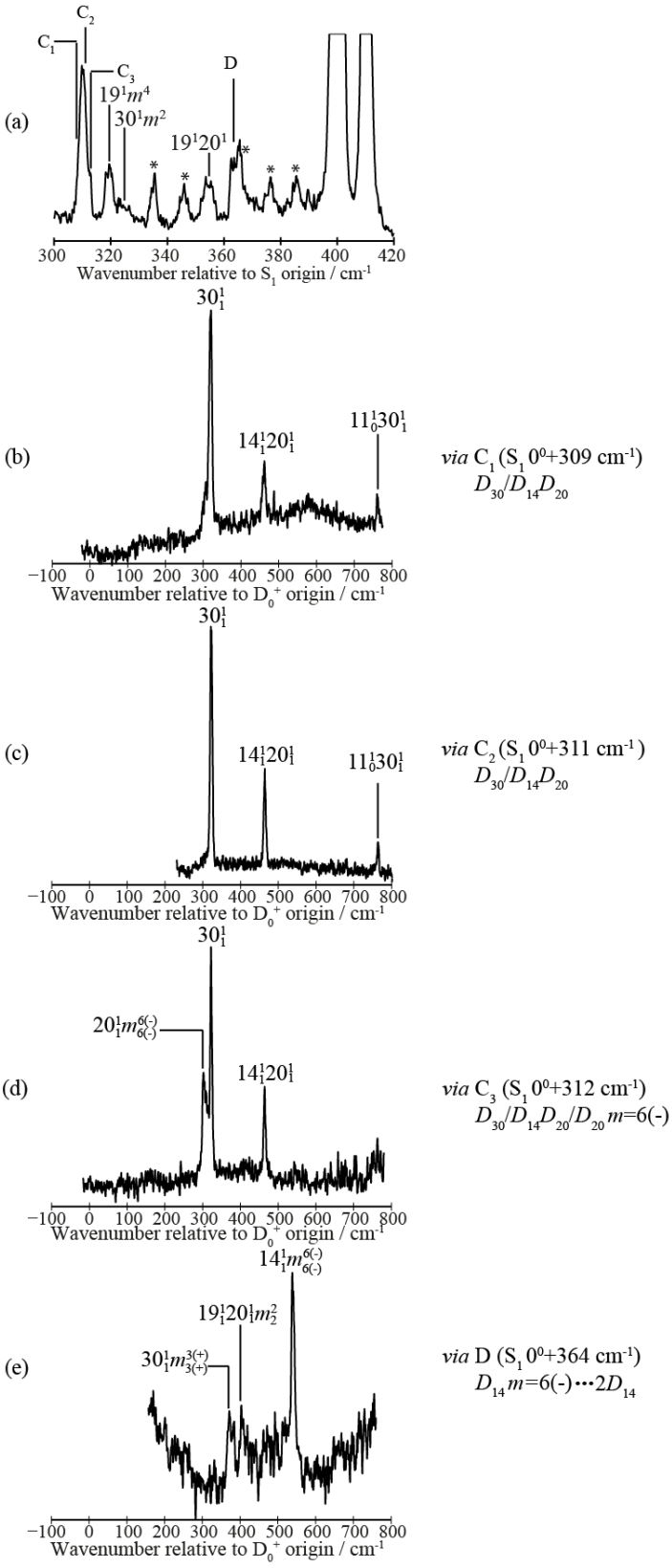
(a)
C1
C2
C3
19¹m⁴
30¹m²
19¹20¹
D
Wavenumber relative to S1 origin / cm-1
(b)
30¹1
14¹120¹1
11¹030¹1
via C1 (S1 0⁰+309 cm-1)
D30/D14D20
(c)
via C2 (S1 0⁰+311 cm-1)
D30/D14D20
(d)
20¹1m⁶(-)6(-)
via C3 (S1 0⁰+312 cm-1)
D30/D14D20/D20 m=6(-)
(e)
14¹1m⁶(-)6(-)
19¹120¹1m²2
30¹1m³(+)3(+)
via D (S1 0⁰+364 cm-1)
D14 m=6(-)···2D14
Wavenumber relative to D0+ origin / cm-1

**Figure 11**

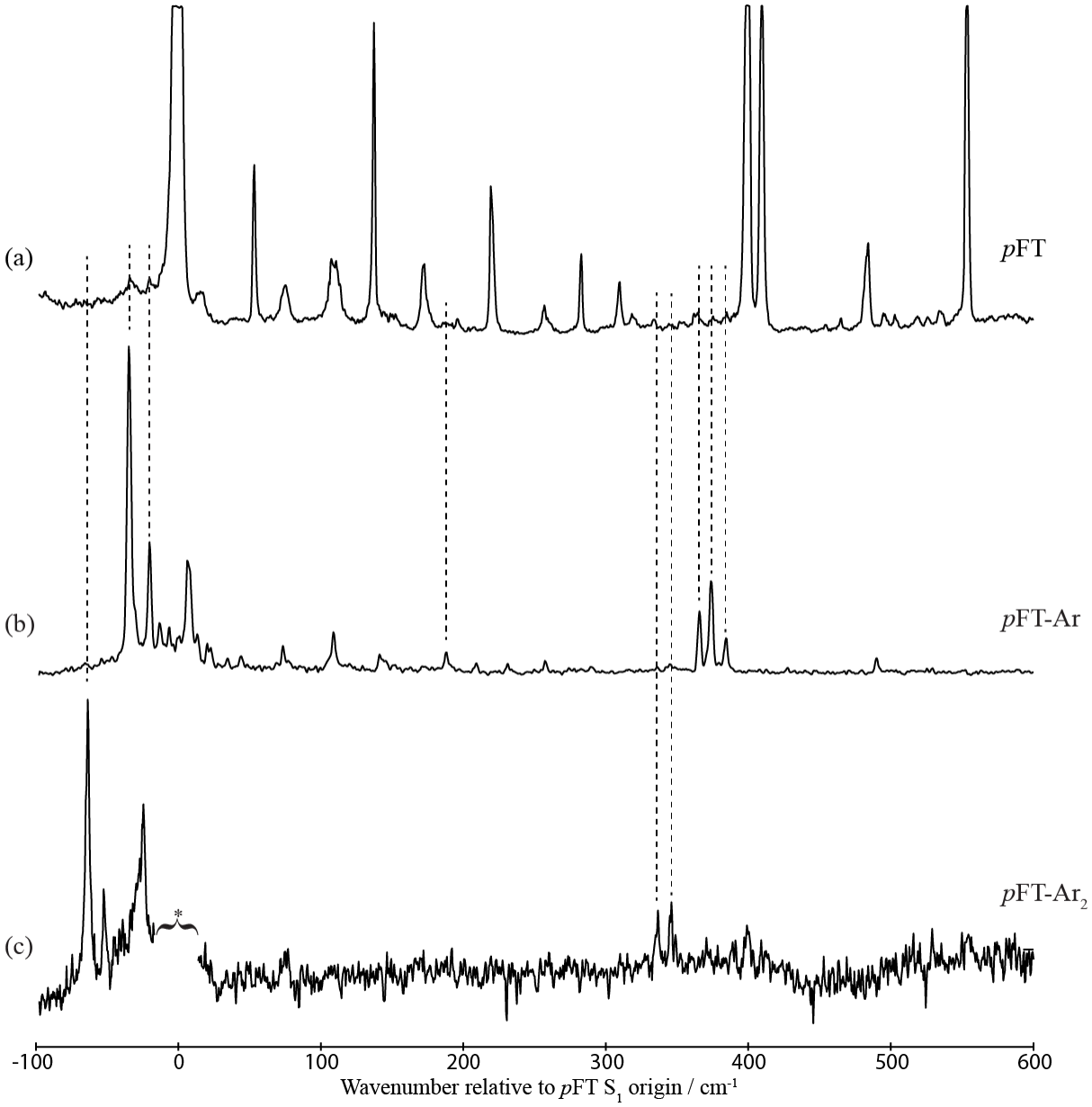
(a)
pFT
(b)
pFT-Ar
(c)
pFT-Ar2
*
-100
0
100
200
300
400
500
600
Wavenumber relative to pFT S1 origin / cm-1

**Figure 12**

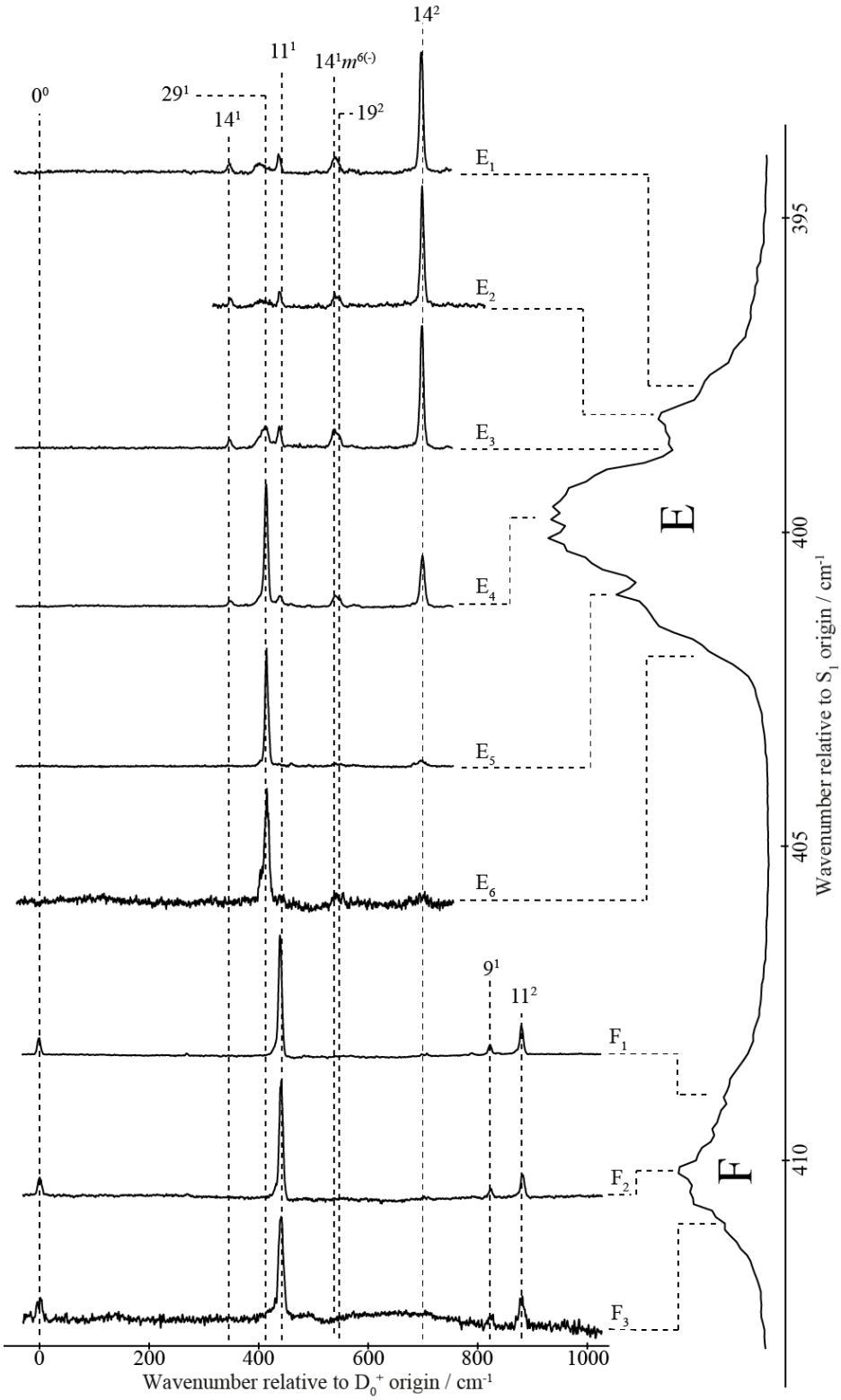
14²
11¹
14¹m⁶(-)
0⁰
29¹
14¹
19²
E1
E2
E3
E4
E5
E6
E
9¹
11²
F1
F2
F3
F
0
200
400
600
800
1000
Wavenumber relative to D0+ origin / cm-1
395
400
405
410
Wavenumber relative to S1 origin / cm-1

**Figure 13**

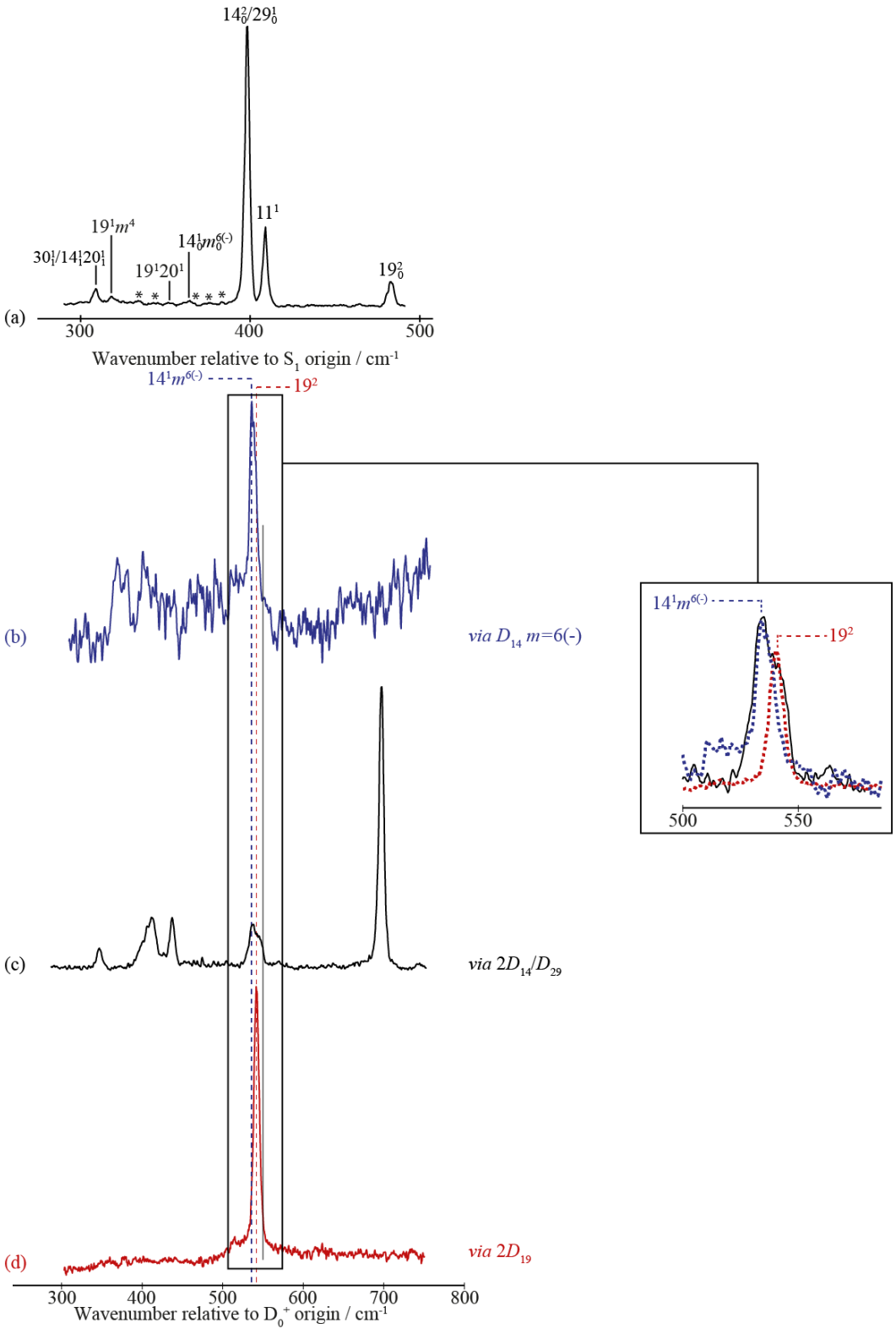
$14_0^2/29_0^1$
$19^1m^4$
$11^1$
$14_0^1m_0^{6(-)}$
$30_1^1/14_1^120_1^1$
$19^120^1$
$19_0^2$
(a)
300
400
500
Wavenumber relative to $S_1$ origin / $cm^{-1}$
$14^1m^{6(-)}$
$19^2$
(b)
via $D_{14}$ $m$=6(-)
$14^1m^{6(-)}$
$19^2$
500
550
(c)
via $2D_{14}/D_{29}$
(d)
via $2D_{19}$
300
400
500
600
700
800
Wavenumber relative to $D_0^+$ origin / $cm^{-1}$

## References


[1] C. S. Parmenter and B. M. Stone, J. Chem. Phys. **84**, 4710 (1986).

[2] Y. He, C. Wu, and W. Kong, J. Phys. Chem. A **107**, 5145 (2007).

[3] C. Skinnerup Byskov, F. Jensen, T. J. D. Jørgensen, and S. Brøndsted Nielsen, Phys. Chem. Chem. Phys. **16**, 15831 (2014).

[4] J. Murakami, M. Ito, and K.Kaya, Chem. Phys. Lett. **80**, 203 (1981).

[5] P. J. Breen, J. A. Warren, E. R. Bernstein, and J. I. Seeman, J. Chem. Phys. **87**, 1917 (1987).

[6] C. G. Hickman, J. R. Gascooke, and W. D. Lawrance, J. Chem. Phys. **104**, 4887 (1996).

[7] D. R. Borst and D. W. Pratt, J Chem. Phys. **113**, 3658 (2000).

[8] A. M. Gardner, A. M. Green, V. M. Tamé-Reyes, V. H. K. Wilton, and T. G. Wright, J. Chem. Phys. **138**, 134303 (2013).

[9] A. M. Gardner, A. M. Green, V. M. Tamé-Reyes, K. L. Reid, J. A. Davies, V. H. K. Wilton, and T. G. Wright, J. Chem. Phys. **140**, 114038 (2014).

[10] A. M. Gardner and T. G. Wright, J. Chem. Phys. **135**, 114305 (2011).

[11] J. R. Gascooke and W. D. Lawrance, J. Chem. Phys. **138**, 134302 (2013).

[12] J. A. Davies, A. M. Green, and K. L. Reid, Phys. Chem. Chem. Phys. **12**, 9872 (2010).

[13] J. A. Davies, A. M. Green, A. M Gardner, C. M. Withers, T. G. Wright, and K. L. Reid, Phys. Chem. Chem. Phys. **16**, 430 (2014).

[14] J. R. Gascooke, E. A. Virgo, and W. D. Lawrance, J. Chem. Phys. **143**, 044313 (2015).

[15] R. J. Doyle, E. S. J. Love, R. Da Campo, and S. R. Mackenzie, J. Chem. Phys. **122**, 194315 (2005).

[16] J. R. Gascooke, E. A Virgo, and W. D. Lawrance, J. Chem. Phys. **142**, 024315 (2015).

[17] J. R. Gascooke and W. D. Lawrance, J. Mol. Spect. **318**, 53 (2015).

[18] K.-T. Lu, G. C. Eiden, and J. C. Weisshaar, J. Phys. Chem. **96**, 9742 (1992).

[19] F. Gunzer and J. Grotemeyer, Phys. Chem. Chem. Phys. **4**, 5966 (2002).

[20] A. Held, H. L. Selzle, and E. W. Schlag, J. Phys. Chem. A **102**, 9625 (1998).

[21] C. J. Seliskar, M. A. Leugers, M. Heaven, and J. L. Hardwick, J. Mol. Spect. **106**, 330 (1984).

[22] A. E. W. Knight and S. H. Kable, J. Chem. Phys. **89**, 7139 (1988).

[23] D. A. Dolson, C. S. Parmenter, and B. M. Stone, Chem. Phys. Lett. **81**, 360 (1981).

[24] D. B. Moss, C. S. Parmenter, and G. E. Ewing, J. Chem. Phys. **86**, 51 (1987).

[25] Q. Ju, C. S. Parmenter, T. A. Stone, and Z.-Q. Zhao, Isr. J Chem. **37**, 379 (1997).

[26] J. A. Davies, K. L. Reid, M. Towrie, and P. Matousek, J. Chem. Phys. **117**, 9099 (2002).

[27] A. K. King, S. M. Bellm, C. J. Hammond, K. L. Reid, M. Towrie, and P. Matousek, Mol. Phys. **103**, 1821 (2005).

[28] J. A. Davies and K. L. Reid, J. Chem. Phys. **135**, 124305 (2011).

[29] J. A. Davies and K. L. Reid, Phys. Rev. Lett. **109**, 193004 (2012).

[30] K. Okuyama, N. Mikami, and M. Ito, J. Phys. Chem. **89**, 5617 (1985).

[31] Z.-Q. Zhao, C. S. Parmenter, D. B. Moss, A. J. Bradley, A. E. W. Knight, and K. G. Owens, J. Chem. Phys. **96**, 6362 (1992).

[32] Z.-Q. Zhao, PhD Thesis, Indiana University (1992).

[33] S. Georgiev, T. Chakraborty, and H. J. Neusser, J. Phys. Chem. A **108**, 3304 (2004).

[34] Y. Hu, X. Wang, and S. Yang, Chem. Phys **290**, 233 (2003).

[35] Z.-Q. Zhao and C. S. Parmenter, *Mode Selective Chemistry* (Kluwer, 1991) Eds. J. Jortner, R. D. Levine, and B. Pullman. Jerusalem Symp. Quant. Chem. Biochem. **24**, 127 (1991).

[36] K. Takazawa, M. Fujii, and M. Ito, J. Chem. Phys. **99**, 3205 (1993).

[37] V. L. Ayles, C. J. Hammond, D. E. Bergeron, O. J. Richards, and T. G. Wright, J. Chem. Phys. **126**, 244304 (2007).

[38] J. R. Gascooke, W. D. Lawrance, and L. Stuart, manuscript in preparation.

[39] J. R. Gascooke, W. D. Lawrance, L. Stuart, A. M. Gardner, W. D. Tuttle, and T. G. Wright, manuscript in preparation.

[40] A. Andrejeva, A. M. Gardner, W. D. Tuttle, and T. G. Wright J. Mol. Spect. **321**, 28 (2016).

[41] G. Varsányi, *Assignments of the Vibrational Spectra of Seven Hundred Benzene Derivatives* (Wiley, New York, 1974).

[42] E. B. Wilson, Jr, Phys. Rev. 45 (1934) 706.

[43] P. R. Bunker and P. Jensen, *Molecular Symmetry and Spectroscopy*, 2nd Ed. (NRCC, Ottawa, Canada, 1998).

[44] R. A. Walker, E. Richard, K.-T. Lu, E. L. Sibert III, and J. C. Weisshaar, J. Chem. Phys. **102**, 8718 (1995).

[45] E. A. Virgo, J. R. Gascooke, and W. D. Lawrance, J. Chem. Phys. **140**, 154310 (2014).

[46] A. E. W. Knight and S. H. Kable, J. Chem. Phys. **89**, 7139 (1988).

[47] G. Herzberg, Molecular Spectra and Molecular Structure III. Electronic Spectra and Electronic Structure of Polyatomic Molecules (Krieger, Malabar, 1991).

[48] J. M. Hollas, High Resolution Spectroscopy (John Wiley and Sons, Chichester, 1998).

[49] T. G. Blease, R. J. Donovan, P. R. R. Langridge-Smith, and T. R. Ridley, Laser Chem. **9**, 241 (1988).

[50] J. G. Philis, Chem. Phys. Lett. **169**, 460 (1990).

[51] S. D. Gamblin, S. E. Daire, J. Lozeille, and T. G. Wright, Chem. Phys. Lett. 325, , 232 (2000).

[52] C. J. Hammond, V. L. Ayles, D. E. Bergeron, K. L. Reid, and T. G. Wright, J. Chem. Phys., **125**, 124308 (2006).

[53] X. Zhang, J. M. Smith, and J. L. Knee, J. Chem. Phys. **97**, 2843 (1992).

[54] G. Reiser, D. Rieger, T. G. Wright, K. Muller-Dethlefs, and E. W. Schlag, J. Phys. Chem. **97**, 4335 (1993).

[55] W. D. Tuttle, A. M. Gardner,, L. Whalley, K. B. O'Regan, and T. G. Wright, manuscript in preparation.

[56] W. D. Tuttle, A. M Gardner, K. B. O' Regan, W. Malewicz, J. H. Carter, and T. G Wright, manuscript in preparation.

[57] K.-T. Lu and J. C. Weisshaar, J. Chem. Phys. **99**, 4247 (1993).

[58] Q. Ju, C. S. Parmenter, T. A. Stone, and Z.-Q. Zhao, Isr. J. Chem. **37**, 379 (1997).

[59] J. P. Harris, A. Andrejeva, W. D. Tuttle, I. Pugliesi, C. Schriever, and T. G. Wright, J. Chem. Phys., **141**, 244315 (2014).

[60] A. Andrejeva, W. D. Tuttle, J. P. Harris, and T. G. Wright, J. Chem. Phys. **143**, 104312 (2015).

[61] A. Andrejeva, W. D. Tuttle, J. P. Harris, and T. G. Wright, J. Chem. Phys. **143**, 244320 (2015).

[62] R. A. Walker, E. C. Richard, K.-T. Lu, and J. C. Weisshaar, J.Phys. Chem. **99**, 12422 (1995).

[63] I. Pugliesi, N. M. Tonge, and M. C. R. Cockett, J. Chem. Phys. **129**, 104303 (2008).

[64] See supplementary material at http://dx.doi.org/xxxx for a summary of the wavenumbers and assignments of the ZEKE bands seen when exciting through various $S_1$ intermediate states.